Seasonal changes in the zooplankton community and population structure in the northern Bering Sea from June to September, 2017

Fumihiko Kimura[a,*], Yoshiyuki Abe[b,c], Kohei Matsuno[a,d], Russell R. Hopcroft[e], Atsushi Yamaguchi[a,d]

[a]*Faculty/Graduate School of Fisheries Sciences, Hokkaido University, 3−1−1 Minato-cho, Hakodate, Hokkaido 041-8611, Japan*

[b]*Atmosphere and Ocean Research Institute, The University of Tokyo, 5-1-5 Kashiwanoha, Kashiwa, Chiba 277-8564, Japan*

[c]*Research Development Section, Office for Enhancing Institutional Capacity, Hokkaido University, Kita 21, Nishi 10, Kita-ku, Sapporo, Hokkaido 001-0021, Japan*

[4]*Arctic Research Center, Hokkaido University, Kita-21 Nishi-11 Kita-ku, Sapporo, Hokkaido, 001-0021, Japan*

[5]*Institute of Marine Science, University of Alaska, Fairbanks, AK99775-7220, USA*

*Corresponding author. Tel: 81-138-40-5543; Fax: 81-138-40-5542

E-mail address: f.kimura@fish.hokudai.ac.jp (F. Kimura)

ABSTRACT

Zooplankton community structure in the northern Bering Sea may change significantly over relatively short periods due to the inflow of different water masses and the seasonal release of meroplankton, although details of these changes are still unclear. We studied the zooplankton community in the northern Bering Sea from June to September of 2017 and examined seasonal changes in the community structure and stage

structure of the dominant species. Zooplankton abundance ranged from 41,000 to 928,000 ind. m^{-2}, with the greatest abundances near 174˚W during July. Copepods were the dominant taxa, comprising 10–98% of zooplankton abundance, with benthic larvae such as bivalves dominant at some stations during July and August. Cluster analysis of abundances divided the station/zooplankton communities into seven groups. West of 172˚W, clear seasonal changes were not observed, because the Bering Chukchi Winter Water persisted in the deep layer and sampling was only conducted in this region in July and August. In contrast, the community structures east of 172˚W differed every month due to water masses changes, meroplankton release, and copepod production associated with the phytoplankton bloom. Despite the changes of water mass, development for the dominant large copepods (*Calanus glacialis/marshallae, Eucalanus bungii* and *Metridia pacifica*) was revealed from their population stage structures. Seasonal shifts in species within *Neocalanus* and appendicularians were driven by water mass exchanges. This study demonstrates that zooplankton community in the northern Bering Sea varies substantially on a monthly time scale. Therefore, to evaluate the impact of climate change on zooplankton, it is important to consider both the seasonal period and the dominant water masses present.

Keywords Northern Bering Sea, Seasonal changes, Zooplankton community, Population structure, Copepods, Chaetognaths, Appendicularians

1. Introduction

The northern Bering Sea is a shallow shelf-sea with a depth of approximately 50 m connecting the Arctic Ocean to the remainder of the Bering Sea. It has high productivity that supports zooplankton, benthos, fish, marine mammals and seabirds due to its massive phytoplankton blooms (Springer et al., 1989; Springer and McRoy, 1993; Springer et al., 1996). In recent years, the magnitude and timing of the phytoplankton bloom has changed with the timing of the sea-ice retreat (Fujiwara et al., 2016). For instance, the timing of the sea-ice retreat was approximately two weeks earlier in 2018 than in previous years, influencing the marine ecosystem; the magnitude of the bloom caused by ice algae was small and zooplankton abundance decreased (Cornwall, 2019; Fukai et al., 2019). Decreased sea ice also diminished the deep cold pool (< 2 °C) south of St. Lawrence Island and fish shifted northward and their abundance decreased in the region (Cornwall, 2019; Duffy-Anderson et al., 2019). Thus, the marine ecosystem of the northern Bering Sea is facing rapid changes with sea-ice variations (Huntington et al., 2020).

The area has a complicated hydrographic environment due to the inflow of multiple currents with different hydrographic features. Three types of water masses enter this region from the south (Springer et al., 1989; Danielson et al., 2017) and are defined largely by salinity: Alaskan Coastal Water (ACW; S>31.8), Bering Shelf Water (BSW; 31.8 <S< 32.5) and Anadyr Water (AW; S<32.5) (Coachman et al., 1975). Since zooplankton communities differ in each water mass (Springer et al., 1989), community composition changes longitudinally in this region (Ozaki and Minoda, 1996). Focusing on particular species, the appendicularians *Oikopleurea labradoriensis* and *O.*

69 *vanhoeffeni* may be indicators of Anadyr Water and Bering Shelf Water, respectively,
70 because their original distributions were different within the Bering Sea (Shiga, 1982,
71 Shiga, 1993a, 1993b). By contrast, Pacific copepods input to the northern Bering shelf
72 are governed by the transport volume of Anadyr Water (Springer et al. 1989).

73 On the other hand, species composition of the zooplankton communities can
74 change significantly with water mass and the sudden appearance of meroplankton
75 (Matsuno et al., 2011; Eisner et al., 2013). Barnacle larvae are often the dominant
76 meroplankton on the Bering Sea Shelf where they may exceed 90% of zooplankton
77 abundance (Matsuno et al., 2011). With a planktonic period of only 2–3 weeks (Herz,
78 1933), meroplankton can change the zooplankton community structure within a short
79 period. During the phytoplankton bloom in the Chukchi Sea, sudden increases in
80 meroplankton abundance can change the zooplankton community structure in a period of
81 weeks (Questel et al., 2013). The large seasonal variations in the zooplankton community
82 prevent accurate evaluation of interannual changes compared to sea-ice extent in the
83 Chukchi Sea (Ershova et al. 2015a). In addition, despite reports that water masses change
84 seasonally at Bering Strait (Woodgate et al., 2010), most studies of the zooplankton
85 community in this region are based on snapshot observations. To overcome these
86 problems, at least monthly sampling is needed. The use of inconsistent plankton net mesh
87 sizes by researchers has hampered prior attempts to examine seasonality, but the recent
88 panArctic adoption of the 150-µm mesh (Gill et al., 2011) by many researchers is
89 resolving this limitation (e.g. Hopcroft et al., 2010; Ershova et al., 2015b).

90 In this study, we collected zooplankton samples using plankton nets with 150-
91 µm mesh in the northern Bering Sea during 2017 to examine seasonal changes in the
92 structure of the zooplankton community. Hydrographic data and zooplankton samples

were collected each month from June to September (a total of 4 times). Zooplankton community composition and its association with station location were analyzed. The development and reproduction of copepods, chaetognaths and appendicularians were evaluated based on seasonal changes in their population structure.

2. Materials and methods

A total of 24 zooplankton collections were taken by the T/S Oshoro-Maru, R/V Mirai, and R/V Sikuliaq in the northern Bering Sea (63˚-65˚75′N, 168˚09′-174˚05′W) during June 23–25, July 11–22, August 26–27 and September 20, 2017 (Fig. 1, Table 1). Zooplankton samples were collected by vertical tows with a NORPAC net (mouth diameter: 45 cm; mesh size: 150 μm) or twin ring nets (mouth diameter: 60 cm; mesh size: 150 μm) from 5 m above the bottom to the surface during either day or night. The volume of water filtered through the net was estimated using a one-way flow meter mounted in the mouth of the net. Zooplankton samples were immediately preserved using 5% v/v borax buffered formalin. At all stations, temperature, salinity and fluorescence were measured using vertical casts of a CTD (Sea-Bird Electronics Inc., SBE 911 Plus) and a fluorometer package (Model FLRTD by Wetlabs Inc. or Fluorometer by Seapoint Sensors, Inc.). Water masses were classified by salinity according to Coachman et al. (1975).

Post cruise, zooplankton samples were split using a box splitter (Motoda, 1959). Zooplankton in the aliquots were identified and enumerated under a dissecting microscope. Calanoid copepods were identified to species and copepodid stage level.

117 Identification of copepods followed Brodsky (1967), *Calanus glacialis* and *Calanus*
118 *marshallae* were treated as *C. glacialis/marshallae* in this study because of the difficulty
119 of species level identification (Frost, 1974). Gonad maturation for adult females of the
120 dominant copepod species was evaluated as stage I (immature), stage II (small oocytes in
121 the ovary or oviduct) and stage III (large eggs or distended opaque in oviduct) (Miller et
122 al., 1984; Miller and Clemons, 1988; Niehoff, 1998). Mean Copepodid Stage (*MCS*) of
123 the dominant large copepods (*C. glacialis/marshallae, Eucalanus bungii* and *Metridia*
124 *pacifica*) was calculated using the following equation:

125 $$MCS = \frac{\sum_{i=1}^{6} i \times Ai}{\sum_{i=1}^{6} Ai}$$

126 where i (1–6 indicate C1–C6) indicates the copepodid stage for a species, Ai (ind. m^{-2}) is
127 the abundance of a copepodid stage (cf. Marin, 1987). Total lengths (TL, mm), from the
128 top of the head to the end of the body without the caudal fin, of the dominant chaetognath.
129 *Parasagitta elegans* was measured using calipers for large specimens (TL ≥ 10 mm) or
130 an ocular micrometer for small specimens (TL < 10 mm) to a precision of 0.1 mm. Based
131 on gonadal maturation, *P. elegans* was classified into five stages: juvenile, stages I, II, III,
132 and IV (Terazaki and Miller, 1986). The identification of appendicularians followed Shiga
133 (1993a) and Choe and Deibel (2008). The trunk length of *Oikopleura* spp. was measured
134 with a precision of 0.1 mm using an ocular micrometer under a stereomicroscope.

135 The nonparametric Mann-Whitney U test was carried out to test whether there
136 were significant difference in abundance (total abundance, copepod abundance and
137 euphausiid abundance) between day and night sampling times. This analysis was carried
138 out using Statview (SAS Institute Inc.). Abundance data (X: ind. m^{-2}) for each species
139 were transformed to the fourth-root (X^{-4}) prior to cluster analysis in order to reduce the
140 bias of abundant species. Similarities between samples were examined using the Bray-

141 Curtis index according to differences in species composition. For grouping samples
142 similarity indices were coupled with hierarchical agglomerative clustering and the
143 complete linkage method (unweighted pair group method using arithmetic mean:
144 UPGMA). Nonmetric multidimensional scaling (NMDS) ordination was carried out to
145 delineate the sample groups on a two dimensional map. Multiple regression analysis was
146 carried out for dependent hydrographic variables (latitude, longitude, depth, mean water
147 column temperature, mean water column salinity and integrated water column
148 fluorescence (the summation of the fluorescence values from the water column) and two
149 dimensional NMDS as independent variables. PERMANOVA was carried out to
150 determine the variables that significantly affected cluster grouping. These included
151 sampling day, water mass and their interaction. The analyses were carried out using
152 Primer7 software (PRIMER-E Ltd.). Intergroup differences in the abundance of each
153 species and zooplankton taxon were tested with one-way ANOVA. If the ANOVA
154 identified statistically significant differences ($p < 0.05$), a Tukey-Kramer post hoc test
155 was carried out to clarify the interaction between groups. To clarify the factors that
156 governed the *MCS* of the dominant large copepods (*C. glacialis, E. bungii* and *M.*
157 *pacifica*), an analysis of covariance (ANCOVA) was performed using Statview (SAS
158 Institute Inc.), with the day of the year and water mass as independent variables. A cohort
159 analysis was made of *P. elegans* TL data with the aid of Microsoft Excel Solver (Aizawa
160 and Takiguchi, 1999). It is difficult to quantitatively capture euphausiids with nets due to
161 net avoidance (Wiebe et al., 2004). Therefore, euphausiids were not included in
162 population and lifecycle analyses.

3. Results

3.1. Hydrography

We identified three water masses in our study. Anadyr Water (AW, >32.5 salinity) was present every month, but dominated all layers during June and in the eastern region during July. Bering Shelf Water (BSW, 31.8–32.5 salinity) was observed every month, particularly at depth for the western stations during July and August. Alaskan Coastal Water (ACW, salinity <31.8) was seen at the surface in the Bering Strait (stn. OS5) and west of St. Lawrence Island during July (stn. 16–24), during August (stn. MR1 and MR2), and at the surface of stn. MR109 during September. Water temperature in the study ranged from -1.4 to 10.1 °C. A thermocline was present at approximately 20 m depth during July and August and was particularly strong to the west of 172˚W. Salinity ranged from 31.3 to 32.9 and was freshest in the surface layer west of 172˚W. Chlorophyll fluorescence ranged from 0.09 to 4.94, with a phytoplankton bloom (> 4) in the upper half of the water column occurring to the east of 172˚W during August and September (Figs. 2 and 3).

3.2. Zooplankton community

The zooplankton community composition changed every month with abundances ranging from 41,127 to 927,498 ind. m^{-2}. According to the U-test, there was no significant difference in abundance (total abundance, copepod and euphausiid abundance) between day and night. During June, abundances were similar between

187 stations (144,436–268,357 ind. m^{-2}) except stn. CBW15 that was dominated by Anadyr
188 Water. The zooplankton community structure there was dominated by copepods,
189 copepod nauplii and polychaeta (Fig. 4). During July, abundances varied greatly between
190 stations, the greatest (927,498 ind. m^{-2}) at 174˚W and the lowest (41,127 ind. m^{-2})
191 northwest of St. Lawrence Island near 172˚W. Copepods still dominated, but bivalvia
192 larva were the most dominant taxa at some of the stations. During August, copepods
193 comprised 98% of zooplankton abundance at the most western station but meroplankton
194 (bivalvia larva, barnacle larva and echinopluteus larva) dominated at the other stations.
195 During September, copepods and copepod nauplii dominated (Fig. 4). Twelve genera of
196 copepods were identified (Table 2). Among these species, *E. bungii*, *M. pacifica*, *N.*
197 *cristatus*, *N. flemingeri* and *N. plumchrus* were categorized as Pacific species.
198 Based on the cluster analysis of taxa abundance, stations were categorized based
199 on zooplankton communities and separated into seven groups (A–G) at 64 and 70%
200 similarity (Fig. 5a). The environmental variables significantly affecting cluster analysis
201 were longitude, sampling depth, mean water column salinity and integrated water column
202 fluorescence (Fig. 5b). Mean group abundance was the highest for group G and the lowest
203 for group B. Groups A, B, C and F were characterized by the dominance of copepods
204 *Pseudocalanus* spp. and Cyclopoida, while Groups D, E and G were characterized by the
205 dominance of bivalvia and echinopluteus larvae (Fig. 5c). The distributions of each group
206 changed greatly during the year but not west of 172°W during July and August (Fig. 6).
207 To the east of 172°W, Group A occurred during June, Groups A, B and C occurred during
208 July, Groups D and E occurred during August, and Group F occurred during September.
209 On the other hand, to the west of 172°W, Groups C and G occurred during July and
210 August. The hydrography (salinity and temperature) was similar within each group (Fig.

211 7). Note that there were no stations conducted to the west of 172°W in September. The
212 groups observed east of 172°W were mainly distributed in AW. PERMANOVA indicated
213 that sampling day, water mass and their interaction significantly affected the cluster
214 grouping (Table 3).

215 The one-way ANOVA test for intergroup differences identified the characteristic
216 taxa within each station group (Table 2). Euphausiids were important for Group A,
217 *Oikopleura vanhoeffeni* for Group D, *Acartia* spp. and cladocerans for Group E, and
218 *Calanus* nauplii for Group F. Some species were important in two groups including
219 *Limacina helicina* in Groups B and D, barnacle nauplii in Groups D and E, and
220 *Centropages* spp. in Groups E and F (Table 2).

221

222 *3.3. Copepod population structure*

223

224 The population structures of *C. glacialis/marshallae*, *E. bungii* and *M. pacifica*
225 changed seasonally. For *C. glacialis/marshallae*, *E. bungii* and *M. pacifica*, copepodid
226 stages I (CI) to IV (CIV) were abundant during June and decreased by August. In contrast,
227 copepodid stage V (CV) was dominant during August. All copepodid stages of
228 *Pseudocalanus* spp. appeared throughout the observation period but no clear change
229 occurred in their population structure (Fig. 8).

230 *Calanus* spp. and *Pseudocalanus* spp. nauplii occurred in June, August and
231 September, *Calanus* spp. nauplii were greater in abundance during September and
232 *Pseudocalanus* spp. nauplii were greater during June in the eastern region (Fig. 9). *E.*
233 *bungii* nauplii abundances were greater in June in the eastern region and near 172°W.

234 *C. glacialis/marshallae* adult females occurred in June, August and September

(Fig. 8), and reproductively mature adult females were observed each month (Fig. 10). Adult females of *E. bungii* and *N. flemingeri* occurred only in July, approximately 40–50% of which were reproductively mature. Adult females of *M. pacifica* occurred during every month but reproductively mature females were seen only in September. Adult females of *Pseudocalanus* spp. with a high ratio of reproductively mature females occurred during every month. For *C. glacialis/marshallae, E. bungii* and *M. pacifica*, the association of the mean copepodite stage (*MCS*) with day of the year and water mass type (ACW, BSW, AW) was evaluated using ANCOVA; none were associated with water mass, but all had a positive correlation with day of the year (Table 4, Fig. 11). *MCS* indicated no significant difference within water mass, but large divisions might be affected by the difference in water mass. Notably, development of *C. glacialis/marshallae* was faster from June to July and slower after August when most individuals had reached CV.

Seasonal occurrence of the three species of *Neocalanus* spp. differed among species: *N. cristatus* occurred during June through July, *N. flemingeri* occurred from June to August, and *N. plumchrus* occurred during September (Fig. 12). For these three species, CI-CIII were not observed (Fig. 12). *N. cristatus* was composed of CIV-CV, *N. flemingeri* of CIV, CV, adult male and adult females, and *N. plumchrus* of CIV-CV.

3.4. Chaetognatha

Parasagitta elegans was the predominant chaetognath species with only trace occurrences of *Eukrohnia hamata* at several stations and abundance for the two species ranging from 90–2486 ind. m^{-2} and 0–45 ind. m^{-2}, respectively. *P. elegans* TL separated into one or two cohorts (Fig. 13). The mean TL of each cohort ranged from 2.7 cm (small

cohort in August) to 16.1 cm (large cohort in August). The abundance of smaller individuals was greater in June than in other months. Mature individuals were typically over 22 mm length and occurred during August and September.

3.5. Appendicularia

The appendicularians *Fritillaria* spp., *O. labradoriensis* and *O. vanhoeffeni* occurred in abundances ranging from 0–23,615, 0–4415 and 0–16,345 ind. m^{-2}, respectively. *Fritillaria* spp. was usually the dominant taxon. Species composition and trunk length of *Oikopleura* showed that smaller individuals (less than 1 mm trunk length) predominated (Fig. 14). A clear seasonal change in species composition was observed: *O. labradoriensis* dominated in June and July while *O. vanhoeffeni* dominated in August and September (Fig. 14).

4. Discussion

4.1. Seasonal changes in community structure

Most of the previous studies of zooplankton community in the northern Bering Sea were based on snapshot observations, and these were impossible to examine impact of changing water mass in the short term on the zooplankton community. In this study, by same sampling methods for four straight months, we observed that zooplankton community and population structure for dominant species varies substantially on a monthly time scale in the northern Bering Sea.

283 Separate summer (Springer et al., 1989) and autumn (Pinchuk and Eisner, 2017)
284 communities have been reported previously in the northern Bering Sea, but seasonal
285 changes in zooplankton during each month has not been studied previously. In the
286 southern Chukchi Sea, zooplankton community showed interannual changes with sea-ice
287 reduction and water mass changes (Ershova et al., 2015a) However, the sampling periods
288 were different among the years, creating unclear long-term trends due to large yearly
289 variation. The biomass of Pacific zooplankton carried onto the northern Bering shelf is
290 governed by the volume transport of Anadyr Water (Springer et al., 1989). According to
291 Matsuno et al. (2011), the zooplankton community was changed by increased Pacific
292 Water inflow; however, monthly changes were not explicitly evaluated in that paper.
293 Resolving seasonal variability is critical for evaluation of long-term trends for
294 zooplankton influenced by sea-ice variation and climate change in the northern Bering
295 Sea, as well as in the Chukchi Sea.

296 In the northern Bering Sea, seasonal change patterns for water masses were
297 different east and west of 172˚W. West of 172˚W a two-layer structure was observed with
298 dominance of ACW in the surface layer and BSW in lower layers during July and August.
299 It is unusual for ACW to appear west of St. Lawrence Island. East of 172˚W, AW was
300 dominant at lower depths during all seasons but the water masses in the surface layer
301 changed seasonally.

302 West of 172˚W, only two zooplankton communities (Groups C and G) occurred
303 during July and August. Group G occurred most westerly and showed the highest
304 abundance through the sampling period. In the previous study, it was reported that
305 zooplankton community structure was strongly related to bottom water mass because
306 large-sized zooplankton concentrate in the bottom layer (Coyle et al., 1996; Eisner et al.,

307 2013; Questel et al., 2013; Ershova et al., 2015a, 2015b). Therefore, the zooplankton
308 community of the western region may be affected by cold water masses that occur in the
309 bottom layer in this region. Although not significant, more *C. glacialis/marshallae*
310 occurred in Groups C and G than other groups suggesting that these species are mainly
311 distributed in cold water masses in the bottom layer. In the Bering and Chukchi seas the
312 biomass of *Calanus glacialis* is strongly correlated with Bering Chukchi Winter Water,
313 with temperatures less than 0 °C (Pinchuk and Eisner, 2017). The population migrates
314 down into the lower layer by winter convection (Coyle et al., 1996). Additionally, the
315 towing depth of plankton nets at stations in Group G were deeper than for the other groups
316 (average 67 vs 45 m). Thus, the occurrence of Group G could be associated with a deeper
317 water mass with high zooplankton density and the greater towing depth of the net. In this
318 study, since cold water masses occurred in the bottom layer of the western region during
319 July and August, the community structures of Groups G and C may have been greatly
320 affected by these cold water masses. Therefore, seasonal change in the community was
321 not observed in the western region, presumably because a colder water mass with
322 abundant large copepods (i.e. *C. glacialis/marshallae*) was always present in the bottom
323 layer during July and August.

324 On the other hand, seasonal change in the community structure was clearly
325 observed east of 172˚W. During June through July, Groups A and B contained many
326 Pacific copepods and euphausiids. This is induced by inflow of Anadyr Water, with high
327 salinity and a greater abundance of Pacific copepods and euphausiids (Springer et al.,
328 1989). In August, Group E contained many cladocerans, *Acartia* spp. and *Centropages*
329 spp., characteristic species of ACW (Hopcroft et al., 2010). However, hydrography of the
330 station where Group E occurred had moderate salinity (32.2–32.3) and lower

temperatures (0.5–0.9 °C), suggesting that it was not ACW. Furthermore, because of the vertically similar water mass structure, it is possible that strong vertical mixing was stimulated by wind and small eddies that resulted in a different zooplankton community structure compared to adjacent stations. In addition, there were many appendicularian *O. vanhoeffeni* in Group D, barnacle nauplii in Groups D and E, and the phytoplankton bloom was observed at the same time in these groups. Because *O. vanhoeffeni* occurs mainly in Bering Shelf Water (Shiga, 1993a, 1993b), Group D is believed to have originated from Bering Sea Water. The onset of phytoplankton bloom is a key factor in the timing of barnacle larvae release from benthic adults (Crisp, 1962), consistent with presence of barnacle nauplii concurrent with elevated August phytoplankton concentrations.

In September, Group F occurred with many *Centropages* spp. and *Calanus* nauplii. As mentioned above, *Centropages* spp. is abundant within the ACW, suggesting that a similar water mass inflow occurred during September and August. The reproduction of *C. glacialis* uses mainly energy from feeding (Søreide et al., 2010) with the maximum reproduction rate coincident with the phytoplankton bloom (Niehoff et al., 2002). While the water mass did not change from August to September, the influx of a large number of *C. glacialis* nauplii following the phytoplankton bloom, resulted in a change in the community composition.

The difference between taxa (barnacles vs copepods) in the timing of abundance increases triggered by the phytoplankton bloom is thought to reflect differences in their reproductive timing and growth rates. Thus, barnacles rapidly reproduce releasing nauplii in associated with the phytoplankton bloom (Costlow and Bookhout, 1957; Crisp, 1962), but copepods need time to grow large enough to be collected by nets after reproduction

(Peterson, 1986). In summary, for seasonal changes in the eastern northern Bering Sea the zooplankton community structure changed every month due to differing advection of water masses and different reproductive attributes of copepods and benthos in response to the phytoplankton bloom.

4.2. Reproduction and development of dominant copepods

Based on population structure and nauplii occurrence most of the dominant copepods in this ecosystem developed and reproduced during the sampling period. In terms of their reproductive timing, *C. marshallae* reproduces during early spring (April) in the southeastern Bering Sea (Vidal and Smith, 1986), and *C. glacialis* reproduces during March to June in the Chukchi Sea (Ashjian et al., 2003). It is suggested that *C. glacialis/marshallae* reproduces during a prolonged period in this region because nauplius and reproductively mature adult females occurred from June to September in this study. Their early copepodite stages were most abundant in June then matured throughout the summer so that the CV stage was most abundant in August, suggesting a one-year life cycle in the northern Bering Sea. *Calanus* spp. has a diapause phase in their life cycle, with CV being the diapause stage for *Calanus glacialis/marshallae* in the Bering Sea. Accordingly, delayed development at CV was observed. While the relationship between developmental stage and day of the year is not a general method for evaluating the development of copepods, it has the advantage of using field data directly without incubation experiments. A relational expression in this study (June to August: MCS = 0.0183D ± 0.6215, August to September: MCS = 0.0132D ± 1.786) showed a steeper slope and faster development than previously observed in the Chukchi Sea (MCS

379 = 0.012D ± 0.881, Matsuno et al., 2016). They sampled from July to October in the
380 Chukchi Sea so the difference in rate between these two studies may be due to
381 environmental conditions (temperature, sea-ice coverage) of the sampling region
382 (Chukchi Sea vs northern Bering Sea) or to observational periods.

383 *E. bungii* is mainly distributed in the subarctic North Pacific Ocean, with
384 individuals occurring in the northern Bering Sea thought to be transported there in Anadyr
385 Water (Springer et al., 1989). This species has a one-year or two-year life cycle in the
386 western and eastern North Pacific Ocean, respectively (Miller et al., 1984; Shoden et al.,
387 2005). Reproduction is performed at the surface during the phytoplankton bloom (Miller
388 et al., 1984). The reproductive period of this species varies according to the region, in the
389 Oyashio region in April to May (Tsuda et al., 2004) and in the central Gulf of Alaska from
390 June to July (Miller et al., 1984). In the southeastern Bering Sea, reproduction is during
391 April to May and the early copepodite stages occur in early June (Vidal and Smith, 1986).
392 In this study, nauplii occurred in June, suggesting that reproduction occurred before June
393 in this region. For this species, the development time from egg to C5 is 3–4 months at
394 5 °C based on incubation experiments in the laboratory (Takahashi and Ide, 2011). On the
395 other hand, *Calanus finmarchicus,* distributed in the subarctic Atlantic Ocean, develops
396 from egg to CV in 50 days at 5 °C (Corkett, 1986). Therefore, the development rate of *E.*
397 *bungii* would not be faster than that of *Calanus* spp. at the same temperature based on
398 previous laboratory experiments. However, in this study, development of *E. bungii* was
399 the fastest among the dominant three large-bodied copepods. This might be caused by
400 reproduction before our observation period or input of nauplii and early copepodite stages
401 since many early copepodite stages occurred during June through July. Unfortunately,
402 population development could not be accurately evaluated due to seasonal changes in

403 water masses and low abundances with high variation for this species compared to the
404 other two species.

405 *M. pacifica* is distributed throughout the subarctic North Pacific Ocean and does
406 not have a diapause phase (Padmavati et al., 2004). This species is believed to be
407 transported to the study area in Anadyr Water and Bering Shelf Water because it occurs
408 mainly in Gulf of Anadyr and to the east of St. Lawrence Island (Springer et al., 1989;
409 Ozaki and Minoda, 1996). *M. pacifica* reproduces from March through October, peaking
410 with the spring bloom in the Gulf of Alaska (Hopcroft et al., 2005), develops during
411 summer to autumn, then develops to adult during December to January (Naumenko,
412 1979). It is thought that they reproduce though the observed period because early
413 copepodite stages and adult female occurred during June through September. This species
414 develops during June through August because the population composition of early
415 copepodite stages was highest in June while later copepodite stages dominated during
416 August to September. The development of this species was the slowest among the
417 dominant copepods. This may be due to the continuous occurrence of adult females and
418 reproduction.

419 *Neocalanus* spp. are known to be mainly transported in Anadyr Water (Springer
420 et al., 1989). This genus diapauses at depth, with timing of diapause cessation and CV
421 migration to the surface layer differing between the species: *N. cristatus* in May-July, *N.*
422 *flemingeri* in April, *N. plumchrus* in July (Tsuda et al., 1999; Tsuda et al., 2004). In this
423 study, the timing of the occurrence of *N. plumchrus* was later than for the other two
424 species, with both CV and CIV observed.

425 Four species of *Pseudocalanus* genus are known to occur in the study region
426 (Ershova et al., 2016). *Pseudocalanus acuspes*, dominant in this region (Ershova et al.,

427 2016), spawns throughout all seasons in the Baltic Sea (Renz et al., 2007). In this study,
428 reproduction occurred over the entire observation period with *Pseudocalanus* nauplii
429 occurred during in June through September in the east region. We cannot comment on
430 population dynamics because we did not distinguish species.
431
432 *4.3. Seasonal changes in Chaetognatha*
433
434 Two species of chaetognaths, *P. elegans* and *E. hamata*, were observed between
435 0–150 m, especially *P. elegans*, with a widespread distribution (Kotori, 1976). The species
436 information used to be an index of water mass, but these two species were similarly
437 distributed in the northern Bering Sea. Growth rate of chaetognaths differs regionally
438 from 3–6 mm month^{-1} in the Celtic Sea (Conway and Williams, 1986; Terazaki and Miller,
439 1986), and it varies with temperature (Sameoto, 1971). Unfortunately, it was impossible
440 to estimate growth rate in this study, possibly due to water mass exchanges accompanying
441 different temperatures.
442 The reproduction timing of *P. elegans* varies with region. Reproduction is
443 observed during three times (early summer, autumn and winter) in the eastern North
444 Pacific (Terazaki and Miller, 1986), or two times (from spring to autumn) in the Bedford
445 Basin, Celtic Sea and Canadian Arctic Ocean (Zo, 1973; Conway and Williams, 1986;
446 Grigor et al., 2014, 2017).In this study, because smaller individuals occurred in every
447 month while mature individuals occurred only during August and September, this species
448 reproduced at least in August/September.
449
450 *4.4. Seasonal changes in Appendicularia*

It is known that appendicularians rapidly reproduce by utilizing phytoplankton blooms and that they have a short generation time (Deibel and Lowen, 2012). In this study, while *O. labradoriensis* was abundant in June and July, *O. vanhoeffeni* occurred in August and September. In Conception Bay, Newfoundland, it has been reported that the occurrence of *F. borealis*, *O. labradoriensis* and *O. vanhoeffeni* correspond to variations in prey size arising from changes in the phytoplankton assemblage (Choe and Deibel, 2008). In our study region, seasonal succession of the phytoplankton community and cell-size may be a factor but these were not consistently measured on most cruises. The two species of *Oikopleurea* are distributed in different regions: *O. labradoriensis* occurs in the Bering Basin at depths greater than 200 m (Shiga, 1982) and in the Gulf of Alaska, *O. vanhoeffeni* is distributed in the Bering Shelf Water (Shiga, 1993a, 1993b) and throughout the Arctic Ocean. We presume high abundance of *O. labradoriensis* in June and July was driven by inflow of Anadyr Water, and *O. vanhoeffeni* in August and September by inflow of Bering Shelf water (Shiga, 1993a, 1993b). Although BSW was not dominant during August and September, *O. vanhoeffeni* was increased by their active reproduction accompanying the phytoplankton bloom (Deibel and Lowen, 2012). These results are consistent with the seasonal exchange of water masses as revealed by changes in zooplankton community structure. In other words, it is suggested that appendicularian species composition may change seasonally because of inflows of different water masses and active reproduction associated with rich food conditions in the northern Bering Sea.

5. Conclusions

This study examined seasonal changes in the zooplankton community and population structure for dominant species in the northern Bering Sea from June to September of 2017. Community composition differed regionally and seasonally in association with changes in water mass distribution. In the western region seasonal changes were not observed due to the dominance of BCWW in the bottom layer during July and August. In the eastern region, community structure differed every month due to inflow of different water masses, meroplankton release, and copepod reproduction associated with the phytoplankton bloom. For copepod population structures, *C. glacialis/marshallae*, *E. bungii* and *M. pacifica* showed stage progression during the observation period, differing between species according to their life cycle. These results illustrate that the zooplankton community and the population structure of dominant species changed seasonally due to changes in hydrography (water mass) and primary productivity in the northern Bering Sea. These large seasonal changes in zooplankton between months are important to the evaluation of long-term changes in the region. Evaluating long-term changes including seasonal changes will allow us to more accurately predict changes in marine ecosystems under rapid changes such as changes in the extent of sea ice.

Acknowledgements

We thank the captain, officers, crew and researchers on board the T/S Oshoro-Maru, Hokkaido University, R/V Mirai, JAMSTEC and R/V Sikuliaq, University of

Alaska for their outstanding efforts during the field sampling. This work was partially conducted as part of the Arctic Challenge for Sustainability (ArCS) (Program Grant Number JPMXD1300000000) and Arctic Challenge for Sustainability II (ArCS II) (Program Grant Number JPMXD1420318865). A portion of the study was supported through a Grant-in-Aids for Scientific Research 19H03037(B), 18K14506 (Early Career Scientists), and 17H01483 (A) from the Japanese Society for Promotion of Science (JSPS), as well as the North Pacific Research Board's Arctic program A91-99a and A91-00a.

References

Aizawa, Y., Takiguchi, N., 1999. Consideration of the methods for estimating the age-composition from the length frequency data with MS Excel. Bull. Jpn. Soc. Fish. Oceanogr. 63, 205–214. (in Japanese with English abstract)

Ashjian, C.J., Campbell, R.G., Welch, H.E., Butler, M., Keuren, D.V., 2003. Annual cycle in abundance, distribution, and size in relation to hydrography of important copepod species in the western Arctic Ocean. Deep-Sea Res. I 50, 1235–1261.

Brodsky, K.A., 1967. Calanoida of the Far Eastern Seas and Polar Basin of the USSR. Israel Program Scientific Translation, Jerusalem.

Choe, N., Deibel, D., 2008. Temporal and vertical distributions of three appendicularian species (Tunicata) in Conception Bay, Newfoundland. J. Plankton Res. 30, 969–979.

Coachman, L.K., Aagaard, K., Tripp, R.B., 1975. Bering Strait: The Regional Physical Oceanography. University of Washington Press, Seattle, Washington.

Conway, D.V.P., Williams, R., 1986. Seasonal population structure, vertical distribution and migration of the chaetognath *Sagitta elegans* in the Celtic Sea. Mar. Biol. 93, 377–387.

Corkett, I.J., McLaren, I.A., Sevigny, J-M., 1986. The rearing of the marine calanoid copepods *Calanus finmarchcus* (Gunnerus), *C. glacialis* Jaschnov and *C. hyperboreus* Kroyer with comment on the equiproportional rule. Syllogeus 58, 539–546.

Cornwall, 2019. Vanishing Bering Sea ice poses climate puzzle. Science 364, 616–617.

Costlow, J.D., Bookhout, C.G., 1957. Larval Development of *Balanus eburneus* in the Laboratory. Biol. Bull. 112, 313–324.

532 Coyle, K.O., Chavtur, V.G., Pinchuk, A.I., 1996. Zooplankton of the Bering Sea: a review
533 of the Russian-language literature. In: Mathisen, O.A., Coyle, K.O. (Eds.),
534 Ecology of the Bering Sea: A review of the Russian Literature. University of
535 Alaska Sea Grant College Program Report No. 96-01, pp. 97–133.
536 Crisp, D.J., 1962. Release of larvae by barnacles in response to the available food supply.
537 Anim. Behav. 10, 382–383.
538 Danielson, S.L., Eisner, L., Ladd, C., Mordy, C., Sousa, L., Weingartner, T.J., 2017. A
539 comparison between late summer 2012 and 2013 water masses, macronutrients,
540 and phytoplankton standing crops in the northern Bering and Chukchi Seas.
541 Deep-Sea Res. II 135, 7–26.
542 Deibel, D., Lowen, B., 2012. A review of the life cycle and life-history adaptations of
543 pelagic tumicates to environmental conditions. ICES J. Mar. Sci. 69, 358–369.
544 Duffy-Anderson, J.T., Stabeno, P., Andrews III, A.G, Cieciel, K., Deary, A., Farley, E.,
545 Fugate, C., Harpold, C., Heintz, R., Kimmel, D., Kuletz, K., Lamb, J., Paquin,
546 M., Porter, S., Rogers, L., Spear, A., Yasumiishi, E., 2019. Responses of the
547 Northern Bering Sea and Southeastern Bering Sea Pelagic Ecosystems
548 Following Record-Breaking Low Winter Sea Ice. Geophy. Res. Let. 46, 9833–
549 9842.
550 Eisner, L., Hillgruber, N., Martinson, E., Maselko, J., 2013. Pelagic fish and zooplankton
551 species assemblages in relation to water mass characteristics in the northern
552 Bering and Southeast Chukchi seas. Polar Biol. 36, 87–113.
553 Ershova, E.A., Hopcroft, R.R., Kosobokova, K.N., Matsuno, K., Nelson, R.J., Yamaguchi,
554 A., Eisner, L.B., 2015a. Long-term changes in summer zooplankton
555 communities of the western Chukchi Sea, 1945–2012. Oceanography 28, 100–

115.

Ershova, E.A., Hopcroft, R.R., Kosobokova, K.N., 2015b. Inter-annual variability of summer mesozooplankton communities of the western Chukchi Sea: 2004–2012. Polar Biol. 38, 1461–1481.

Ershova, E.A., Questel, J.M., Kosobokova, K., Hopcroft, R.R., 2016. Population structure and production of four sibling species of *Pseudocalanus* spp. in the Chukchi Sea. J. Plankton Res. 39, 48–64.

Frost, B.W., 1974. *Calanus marshallae*, a New Species of Calanoid Copepod Closely Allied to the Sibling Species *C. finmarchicus* and *C. glacialis*. Mar. Biol. 26, 77–99.

Fujiwara, A., Hirawake, T., Suzuki, K., Eisner, L., Imai, I., Nishino, S., Kikuchi, T., Saitoh, S.-I., 2016. Influence of timing of sea ice retreat on phytoplankton size during marginal ice zone bloom period on the Chukchi and Bering shelves. Biogeosciences 13, 115–131.

Fukai, Y., Matsuno, K., Fujiwara, A., Yamagushi, A., 2019. The community composition of diatom resting stages in sediments of the northern Bering Sea in 2017 and 2018: the relationship to the interannual changes in the extent of the sea ice. Polar Biol. 42, 1915–1922.

Gill, M.J., Crane, K., Hindrum, R., Arneberg, P., Bysveen, I., Denisenko, N.V., Gofman, V., Grant-Friedman, A., Gudmundsson, G., Hopcroft, R.R., Iken, K., Labansen, A., Liubina, O.S., Melnikov, I.A., Moore, S.E., Reist, J.D., Sirenko, B.I., Stow, J., Ugarte, F., Vongraven, D., Watkins, J., 2011. Arctic Marine Biodiversity Monitoring Plan (CBMP-MARINE PLAN). CAFF Monitoring Series Report nr. 3, Akureyri.

Grigor, J.J., Soreide, J.E., Varpe, O., 2014. Seasonal ecology and life-history strategy of the high-latitude predatory zooplankter *Parasagitta elegans*. Mar. Ecol. Prog. Ser. 499, 77–88.

Grigor, J.J., Schmid, M.S., Fortier, L., 2017. Growth and reproduction of the chaetognaths *Eukrohnia hamata* and *Parasagitta elegans* in the Canadian Arctic Ocean: capital breeding versus income breeding. J. Plankton Res. 39, 910–929.

Herz, L.E., 1933. The morphology of the later stages of *Balanus crenatus* Bruguiere. Biol. Bull. 64, 432–442.

Hopcroft, R.R., Clarke, C., Byrd, A.G., Pinchuk, A.I., 2005. The paradox of *Metridia* spp. egg production rates: a new technique and measurements from the coastal Gulf of Alaska. Mar. Ecol. Prog. Ser. 286, 193–201.

Hopcroft, R.R., Kosobokova, K.N., Pinchuk, A.I., 2010. Zooplankton community patterns in the Chukchi sea during summer 2004. Deep-sea Res. II 57, 27–39.

Huntington, H.P., Danielson, S.L., Wiese, F.K., Baker, M., Boveng, P., Citta, J.J., Robertis, A.D., Dickson, D.M.S., Farley, E., George, J.C., Iken, K., Kimmel, D.G., Kuletz, K., Ladd, C., Levine, R., Quakenbush, L., Stabeno, P., Stafford, K.M., Stockwell, D., Wilson, C. 2020. Evidence suggests potential transformation of the Pacific Arctic ecosystem is underway. Nat. Clim. Change, 10, 342–348.

Kotori, M., 1976. The biology Chaetognatha in the Bering Sea and northwestern North Pacific Ocean, with emphasis on *Sagitta elegans*. Mem. Fac. Fish. Hokkaido Univ. 23, 95–183.

Marin, V., 1987. The oceanographic structure of eastern Scotia Sea-IV. Distribution of copepod species in relation to hydrography in 1981. Deep-Sea Res. 34A, 105–

121.

Matsuno, K., Yamaguchi, A., Hirawake, T., Imai, I., 2011. Year-to-year changes of the mesozooplankton community in the Chukchi Sea during summers of 1991, 1992 and 2007, 2008. Polar Biol. 34, 1349–1360.

Matsuno, K., Abe, Y., Yamaguchi, A., Kikuchi, T., 2016. Regional patterns and controlling factors on summer population structure of *Calanus glacialis* in the western Arctic Ocean. Polar Sci. 10, 503–510.

Miller, C.B., Clemons, M.J., 1988. Revised Life History Analysis for Large Grazing Copepods in the Subarctic Pacific Ocean. Prog. Oceanogr. 20, 293–313.

Miller, C.B., Frost, B.W., Batchelder, H.P., Clemons, M.J., Conway, R.E., 1984. Life Histories of Large, Grazing Copepods in a Subarctic Ocean Gyre: *Neocalanus plumchrus*, *Neocalanus cristatus*, and *Eucalanus bungii* in the Northeast Pacific. Prog. Oceanogr. 13, 201–243.

Motoda, S., 1959. Device of simple plankton apparatus. Mem. Fac. Fish. Hokkaido Univ. 7, 73–94.

Naumenko, Y.A., 1979. Life cycle of copepods in the southeast of the Bering Sea. Hydrobiological J. 15, 20–22.

Niehoff, B., 1998. The gonad morphology and maturation in Arctic Calanus speacies. J. Mar. Syst. 15, 53–59.

Niehoff, B., Madsen, S.D., Hansen, B.W., Nielsen, T.G., 2002. Reproductive cycles of three dominant *Calanus* species in Disko Bay, West Greenland. Mar. Biol. 140, 567–576.

Ozaki, K., Minoda, T., 1996. On the occurrence of oceanic copepods in the northeastern Bering Sea Shelf during the summer. Bull. Plankton Soc. Japan 43, 107–120.

628 Padmavati, G., Ikeda, T., Yamaguchi, A., 2004. Life cycle, population structure and
629 vertical distribution of *Metridia* spp. (Copepoda: Calanoida) in the Oyashio
630 region (NW Pacific Ocean). Mar. Ecol. Prog. Ser. 270, 181–198.
631 Peterson, W.T., 1986. Development, growth, and survivorship of the copepod *Calanus*
632 *marshallae* in the laboratory. Mar. Ecol. 29, 61–72.
633 Pinchuk, A.I., Eisner, L.B., 2017. Spatial heterogeneity in zooplankton summer
634 distribution in the eastern Chukchi Sea in 2012–2013 as a result of large-scale
635 interactions of water masses. Deep-Sea Res. II 135, 27–39.
636 Questel, J.M., Clarke, C., Hopcroft, R.R., 2013. Seasonal and interannual variation in the
637 planktonic communities of the northeastern Chukchi Sea during the summer and
638 early fall. Cont. Shelf Res. 67, 23–41.
639 Renz, J., Peters, J., Hirche, H., 2007. Life cycle of *Pseudocalanus acuspes* Giesbrecht
640 (Copepoda, Calanoida) in the Central Baltic Sea: II. Reproduction, growth and
641 secondary production. Mar. Biol. 151, 515–527.
642 Sameoto, D.D., 1971. Life History, Ecological Production, and an Empirical
643 Mathematical Model of the Population of *Sagitta elegans* in St. Margaret's Bay,
644 Nova Scotia. J. Fish. Res. Board Can. 28, 971–985.
645 Shiga, N., 1982. Regional and Annual Variations in Abundance of an Appendicularian,
646 *Oikopleura labradoriensis* in the Bering Sea and the Northern North Pacific
647 Ocean during Summer. Bull. Plankton Soc. Japan 29, 119–128.
648 Shiga, N., 1993a. First record of the appendicularian, *Oikopleura vanhoeffeni* in the
649 northern Bering Sea. Bull. Plankton Soc. Japan 39, 107–115.
650 Shiga, N., 1993b. Regional and Vertical Distributions of *Oikopleura vanhoeffeni* on the
651 Northern Bering Sea Shelf in Summer. Bull. Plankton Soc. Japan 39, 117–126.

652 Shoden, S., Ikeda, T., Yamaguchi, A., 2005. Vertical distribution, population structure
653 and lifecycle of *Eucalanus bungii* (Copepoda: Calanoida) in the Oyashio region,
654 with notes on its regional variations. Mar. Biol. 146, 497–511.
655 Søreide, J.E., Leu, E., Berge, J., Graeve, M., Falk-Petersen, S., 2010. Timing of blooms,
656 algal food quality and *Calanus glacialis* reproduction and growth in a changing
657 Arctic. Global Chang. Biol. 16, 3154–3163.
658 Springer, A.M., McRoy, C.P., 1993. The paradox of pelagic food webs in the northern
659 Bering Sea-III. Patterns of primary production. Cont. Shelf Res. 13, 575–599.
660 Springer, A.M., McRoy, C.P., Turco, K.R., 1989. The paradox of pelagic food webs in
661 the northern Bering Sea-II. Zooplankton communities. Cont. Shelf Res. 9, 359–
662 386.
663 Springer, A.M., McRoy, C.P., Flint, M.V., 1996. The Bering Sea Green Belt: shelf-edge
664 processes and ecosystem production. Fish. Oceanogr. 5, 205–223.
665 Takahashi, K., Ide, K., 2011. Reproduction, grazing, and development of the large
666 subarctic calanoid *Eucalanus bungii*: is the spring diatom bloom the key to
667 controlling their recruitment? Hydrobiol. 666, 99–109.
668 Terazaki, M., Miller, C.B., 1986. Life history and vertical distribution of pelagic
669 chaetognaths at Ocean Station P in the Subarctic Pacific. Deep-Sea Res. 33, 323–
670 337.
671 Tsuda, A., Saito, H., Kasai, H., 1999. Life histories of *Neocalanus flemingeri* and
672 *Neocalanus plumchrus* (Calanoida: Copepoda) in the western subarctic Pacific.
673 Mar. Biol. 135, 533–544.
674 Tsuda, A., Saito, H., Kasai, H., 2004. Life histories of *Eucalanus bungii* and *Neocalanus*
675 *cristatus* (Copepoda: Calanoida) in the western subarctic Pacific Ocean. Fish.

676 Oceanogr. 13, 10–20.
677 Vidal, J., Smith, S.L., 1986. Biomass, growth, and development of populations of
678 herbivorous zooplankton in the southeastern Bering Sea during spring. Deep-
679 Sea Res. 33, 523–556.
680 Wiebe, P.H., Ashjian, C.J., Gallager, S.M., Davis, C.S., Lawson, G.L., Copley, N.J., 2004.
681 Using a high-powered strobe light to increase the catch of Antarctic krill. Mar.
682 Biol. 144, 493–502.
683 Woodgate, R.A., Weingartner, T., Lindsay, R., 2010. The 2007 Bering Strait oceanic heat
684 flux and anomalous Arctic sea-ice retreat. Geophys. Res. Lett. 37,
685 L01602.doi:10.1029/2009GL041621.
686 Zo, Z., 1973. Breeding and growth of the chaetognath *Sagitta elegans* in Bedford Basin.
687 Limnol. Oceanogr. 18, 750–756.
688

689 **Figure captions**

690 **Fig. 1.** Locations of the sampling stations in the Northern Bering Sea during June through
691 September, 2017. Color of the circles indicated spatial and vertical distribution
692 of the water mass as defined by Coachman et al. 1975 (cf. Fig. 3).

693 **Fig. 2.** Vertical sections of temperature, salinity and fluorescence across the transects of
694 the Northern Bering Sea during June through September, 2017. Solid triangles
695 indicate the western end of the St. Lawrence Island.

696 **Fig. 3.** T-S diagrams from the Northern Bering Sea during June through September, 2017.
697 Numbers and isolines indicate water density. Data from specific stations
698 identified with labels. ACW: Alaskan coastal water, BSW: Bering Shelf water,
699 AW: Anadyr water (cf. Coachman et al. 1975).

700 **Fig. 4.** Monthly changes in total zooplankton abundance and species composition in the
701 northern Bering Sea during June through September, 2017. Solid triangles
702 indicate the western end of St. Lawrence Island.

703 **Fig. 5.** (a) Dendrogram showing Bray-Curtis similarity results for zooplankton abundance.
704 Eight groups (A-G) were identified at 64 and 70% similarity. (b) Nonmetric
705 multidimensional scaling plots of the seven groups, with arrows indicating
706 directions of environmental parameters. (c) The mean abundance and taxonomic
707 composition of each group; only groups with a high % composition are separated.
708 *Depth*: sampling depth (5 m off of the sea floor), *IF*: integrated water column
709 fluorescence, *MS*: mean water column salinity, *Lon.*: longitude.

710 **Fig. 6.** Horizontal distributions of the seven station groups identified using Bray-Curtis
711 similarity cluster analysis based on zooplankton abundance (cf. Fig. 5a) in the
712 northern Bering Sea during June through September, 2017.

713 **Fig. 7.** T-S diagram with the seven groups identified from Bray-Curtis similarity based
714 on zooplankton abundances (cf. Fig. 5a) in the northern Bering Sea during June
715 through September of 2017. The plot position is mean values in the water column.
716 Circles indicate that the stations were located west of 172°W.
717 **Fig. 8.** Monthly changes in abundance and population structure for the dominant
718 copepods in the northern Bering Sea during June through September, 2017.
719 Horizontal bars below the plots indicate the water masses (ACW, BSW and AW)
720 were present for each station.
721 **Fig. 9.** Monthly changes in abundance of nauplii of the dominant copepods species in the
722 northern Bering Sea during June through September, 2017.
723 **Fig. 10.** Monthly changes in abundance and gonad maturation for adult females of the
724 dominant copepods in the northern Bering Sea during June through September,
725 2017.
726 **Fig. 11.** Relationships between mean copepodite stage and Julian day for the dominant
727 copepods in the northern Bering Sea during June through September, 2017.
728 **Fig. 12.** Monthly changes in abundance and population structure for the *Neocalanus*
729 species in the northern Bering Sea during June through September, 2017.
730 Horizontal bars below the plots indicate the water masses (ACW, BSW and AW)
731 present for each station.
732 **Fig. 13.** Monthly changes in the total length of *Parasagitta elegans* in the northern Bering
733 Sea during June through September, 2017. Numbers in parentheses show total
734 individual measurements. Smooth curves indicate the results of a cohort analysis.
735 **Fig. 14.** Monthly changes in the trunk length of *Oikopleura* spp. in the northern Bering
736 Sea during June through September 2017. Numbers in parentheses show total

individual measurements.

738 Table 1. Zooplankton samples used in this study. All samples were collected with vertical hauls of
739 150-μm mesh size nets but with slightly different net diameters on different vessels (60 cm for *R/V*
740 *Sikuliaq*, 45 cm for *T/S Oshoro-Maru* and *R/V Mirai*).

Date	D/N	Station	Latitude (N)	Longitude (W)	Towed depth (m)	Vesssl
June 23, 2017	Night	CBW15	65˚30′	168˚49′	53	Sikuliaq
June 24, 2017	Day	CBW13	65˚14′	169˚21′	45	Sikuliaq
June 24, 2017	Day	DBO2.4	64˚58′	169˚53′	43	Sikuliaq
June 24, 2017	Day	CBW9	64˚41′	170˚26′	45	Sikuliaq
June 25, 2017	Night	CBW7	64˚25′	170˚58′	40	Sikuliaq
June 25, 2017	Day	CBW5	64˚09′	171˚31′	41	Sikuliaq
June 25, 2017	Day	CBW3	63˚53′	172˚03′	43	Sikuliaq
July 11, 2017	Day	OS5	65˚45′	168˚09′	39	Oshoro-Maru
July 11, 2017	Day	OS6	65˚20′	168˚54′	50	Oshoro-Maru
July 12, 2017	Day	OS7	65˚03′	169˚38′	46	Oshoro-Maru
July 18, 2017	Day	OS16	64˚15′	171˚26′	42	Oshoro-Maru
July 18, 2017	Day	OS17	64˚00′	171˚57′	48	Oshoro-Maru
July 19, 2017	Night	OS18	63˚45′	172˚29′	43	Oshoro-Maru
July 19, 2017	Day	OS19	63˚30′	173˚00′	60	Oshoro-Maru
July 22, 2017	Night	OS24	63˚00′	174˚05′	71	Oshoro-Maru
August 26, 2017	Day	MR1	63˚06′	174˚01′	71	Mirai
August 26, 2017	Night	MR2	63˚52′	172˚18′	50	Mirai
August 27, 2017	Night	MR3	64˚43′	170˚21′	43	Mirai
August 27, 2017	Day	MR4	65˚03′	169˚36′	46	Mirai
August 27, 2017	Day	MR5	65˚16′	169˚03′	48	Mirai
August 27, 2017	Day	MR6	65˚39′	168˚42′	44	Mirai
September 20, 2017	Day	MR109	65˚39′	168˚43′	44	Mirai
September 20, 2017	Day	MR110	65˚16′	169˚03′	48	Mirai
September 20, 2017	Day	MR111	65˚04′	169˚36′	45	Mirai

741
742
743
744

745 Table 2. Comparisons of abundance in the northern Bering Sea during June through September of
746 2017. Values are mean abundance in each group of stations. Differences between groups were tested
747 using one-way ANOVA and the Tukey-Kramer HSD post hoc test. Groups not connected by underlines
748 are significant different ($p < 0.05$). *: $p < 0.05$, **: $p < 0.01$, ***: $p < 0.001$.
749

Species/ Taxon	Groups							One-way Anova	Tukey-Kramer test
	A (9)	B (2)	C (3)	D (3)	E (1)	F (3)	G (3)		
Acartia spp.	174	0	632	0	2397	449	357	***	A G F C E
Calanus glacialis/marshallae	7333	1413	7553	451	599	87	15478	*	F D E B A C G
Calanus spp. nauplii	7460	178	1201	9218	0	23209	1002	***	B G C A D F
Centropages spp.	1766	0	405	6915	8788	22276	0	***	C A D E F
Cyclopoida	64625	31644	17101	8063	10385	64931	53930	NS	
Eucalanus bungii	1119	3813	22	294	749	818	0	*	C D E F A B
Eucalanus bungii nauplii	4872	0	0	0	0	0	0	NS	
Metridia pacifica	10636	800	307	5	50	2069	3375	*	Not detected
Microcalanus spp.	31134	622	69	1283	0	1550	511	NS	
Microsetella spp.	0	0	0	820	799	1387	0	**	Not detected
Neocalanus cristatus	42	44	0	0	0	0	0	NS	
Neocalanus flemingeri	3109	1902	709	41	50	0	279	NS	
Neocalanus plumchrus	0	0	0	0	0	37	0	*	Not detected
Oncaea spp.	0	0	0	5835	799	6578	462	***	G E D F
Paraeuchaeta glacialis	0	0	0	0	0	34	0	NS	
Pseudocalanus spp.	73751	12409	25915	33892	14092	31465	172589	NS	
Pseudcalanus spp. nauplii	5455	0	543	6086	2397	5604	0	NS	
Amphipoda	54	0	46	5	0	0	77	NS	
Barnacle cypris	3401	0	2001	13917	799	143	0	NS	
Barnacle nauplii	10620	836	774	28534	45535	577	0	***	F C B A D E
Bivalvia larvae	4163	1902	10810	104841	40742	17369	135696	*	B A C F E D G
Cladocerans	0	0	527	39	2996	0	0	***	D C E
Clione limacina	25	0	0	0	0	0	0	NS	
Decapod megalops	0	44	0	0	0	0	0	NS	
Decapod zoea	131	0	0	5	0	0	89	NS	
Echinoidea larvae	1780	0	0	0	0	0	0	NS	
Echinopluteus larvae	677	0	532	54466	9586	1076	65864	NS	
Eukrohnia hamata	22	36	6	0	0	0	0	**	Not detected
Euphausiacea	6295	560	256	397	0	0	251	***	G C D B A
Euphausiids nauplii	801	89	0	1102	0	2523	0	NS	
Fish larvae	0	53	0	0	0	0	0	NS	
Fritillaria spp.	5386	0	6960	12688	1598	1617	365	NS	
Hydrozoa	0	0	0	0	0	314	0	NS	
Limacina helicina	335	1058	722	2274	0	465	0	***	A F C B D
Oikopleura labradoriensis	1003	6	2	698	57	40	6	NS	
Oikopleura vanhoeffeni	260	0	2	9329	0	274	0	***	C A F D
Oikopleura spp.	74	0	5	2049	0	294	0	NS	
Parasagitta elegans	646	181	436	1437	387	363	1025	NS	
Polychaeta	25246	1067	1627	9023	11983	1721	36529	NS	
Unidentified nauplii	145	0	0	0	799	0	0	NS	
Total copepods	183478	52826	54457	72903	41104	160494	247982	NS	
Total zooplankton	244543	58658	79163	313708	155586	187271	487885	NS	

750
751
752
753

754 Table 3. Results of PERMANOVA on zooplankton community with day and water mass
755 in the northern Bering Sea during June through September of 2017.

Source	d.f.	SS	*F*-value	*p*-value
Day	10	13720	3.9401	***
Water mass	1	2839.7	4.0547	***
Day × water mass	2	1550.9	3.2373	**

756 d.f., degrees of freedom; SS, sum of squares.

757 ***: $p < 0.001$; **: $p < 0.01$

758

759

760
761
762 Table 4. Result of the ANCOVA for *MCS* of the dominant large copepods with Julian day and water
763 mass (cf. Fig. 7) applied as independent variables.
764

Species	Parameters	d.f.	SS	*F* -value	*p* -value
C.glacialis/marshallae	Water	2	0.205	0.553	N.S.
	Day	1	2.652	14.328	***
	Water × day	2	0.207	0.560	N.S.
	Error	31	5.738		
E.bungii	Water	2	0.546	0.351	N.S.
	Day	1	13.312	17.139	***
	Water × day	2	0.535	0.344	N.S.
	Error	21	16.311		
M.pacifica	Water	2	0.602	0.493	N.S.
	Day	1	6.376	10.446	**
	Water × day	2	0.594	0.486	N.S.
	Error	30	18.312		

765
766
767 d.f., degrees of freedom; SS, sum of squares.
768 N.S., not significant.
769 ***: $p < 0.001$; **: $p < 0.01$
770
771

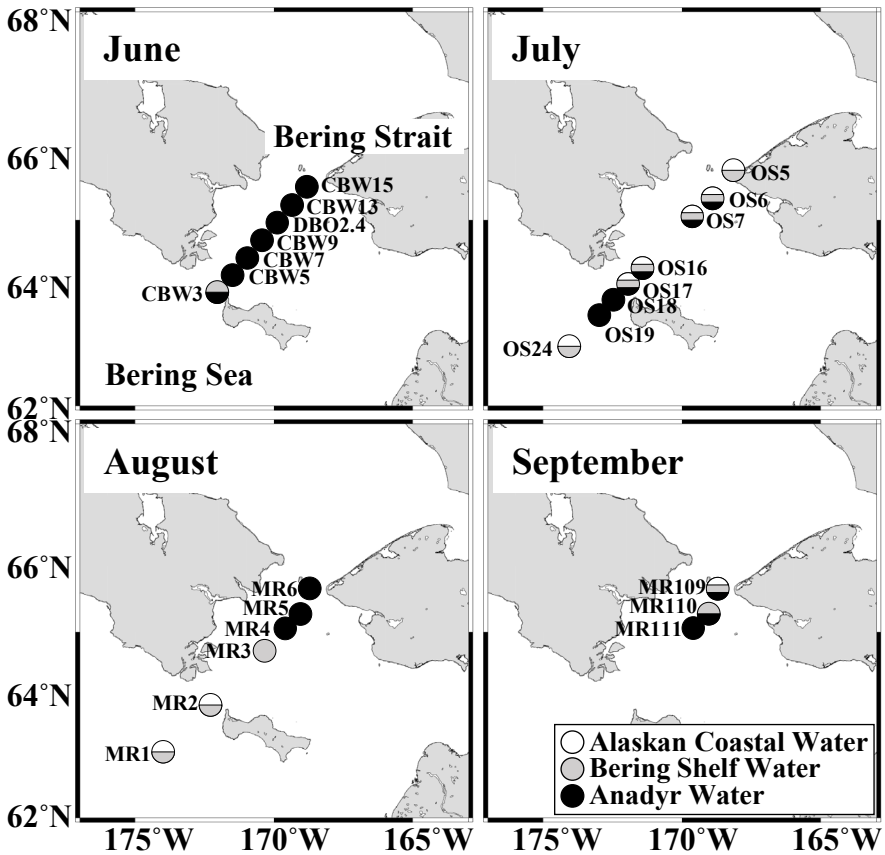

Fig. 1. Locations of the sampling stations in the Northern Bering Sea during June through September, 2017. Color of the circles indicated spatial and vertical distribution of the water mass as defined by Coachman et al. 1975 (cf. Fig. 3).

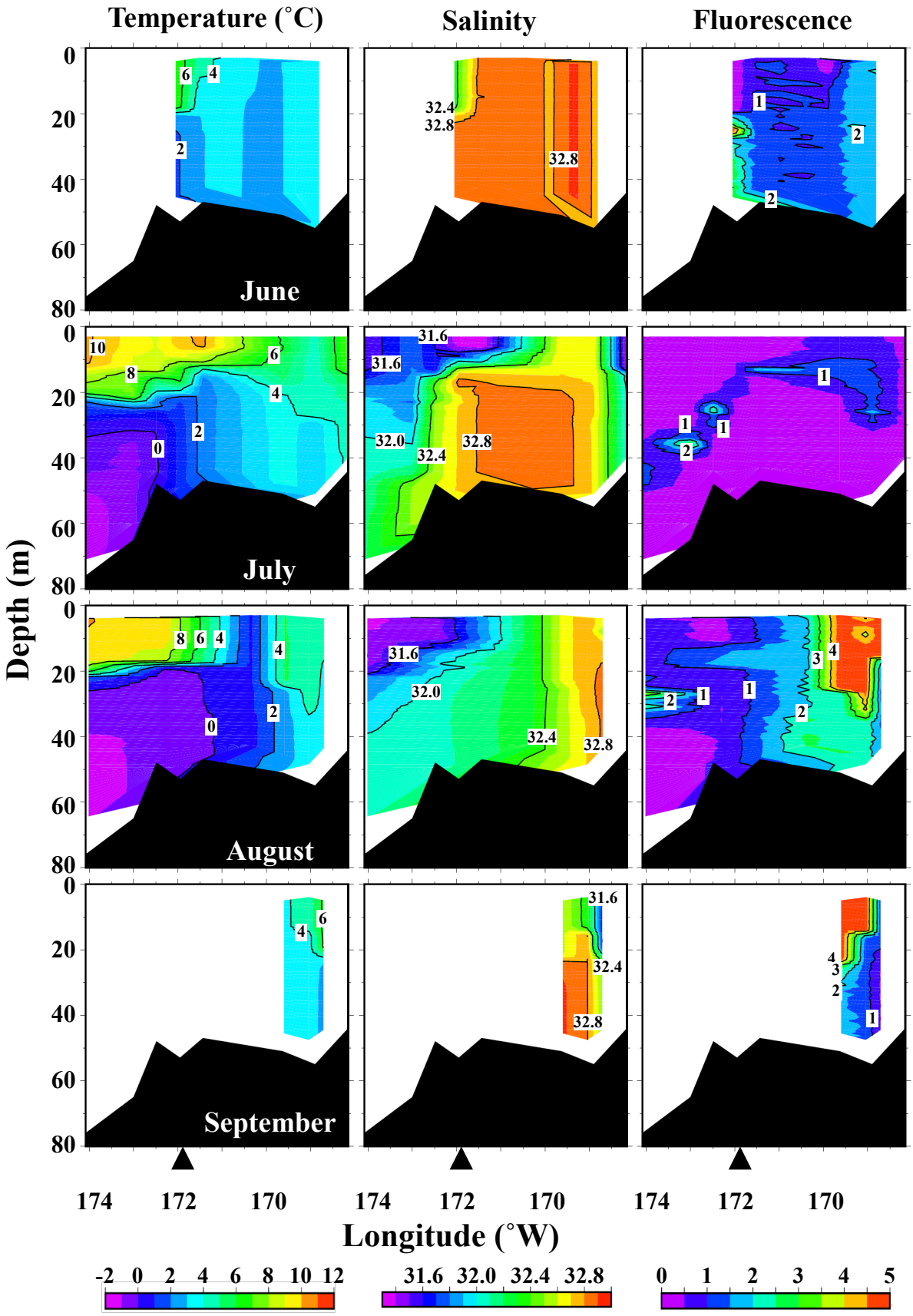

Fig. 2. Vertical sections of temperature, salinity and fluorescence across the transects of the Northern Bering Sea during June through September, 2017. Solid triangles indicate the western end of the St. Lawrence Island.

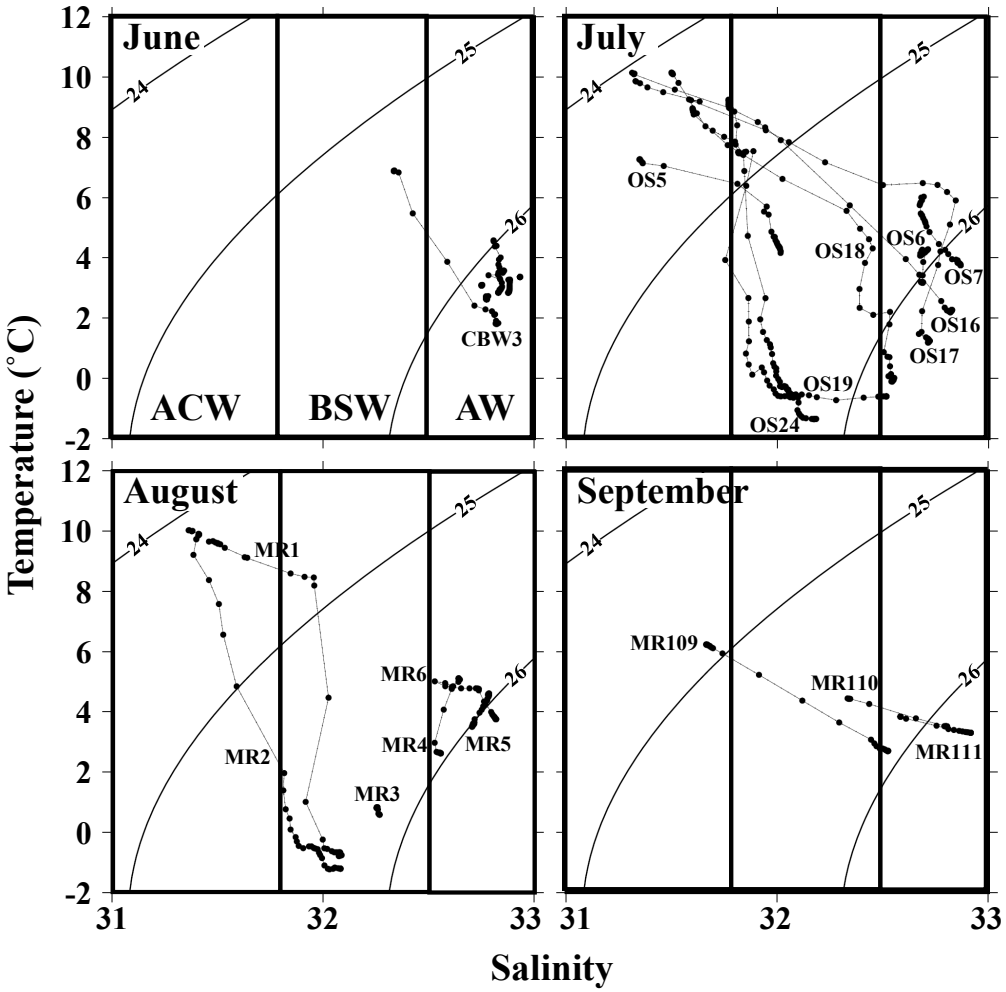

Fig. 3. T-S diagrams from the Northern Bering Sea during June through September, 2017. Numbers and isolines indicate water density. Data from specific stations identified with labels. ACW: Alaskan coastal water, BSW: Bering Shelf water, AW: Anadyr water (cf. Coachman et al. 1975).

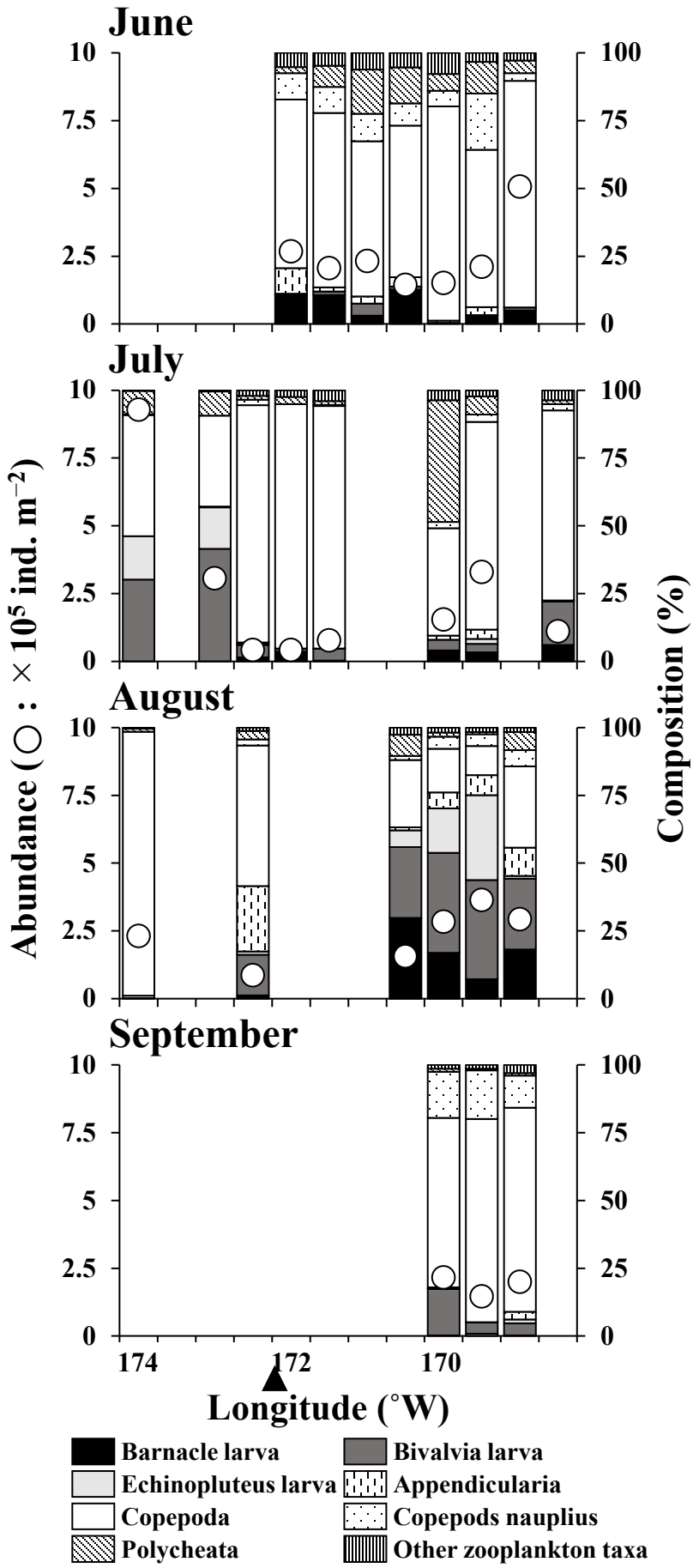

Fig. 4. Monthly changes in total zooplankton abundance and species composition in the northern Bering Sea during June through September, 2017. Solid triangles indicate the western end of St. Lawrence Island.

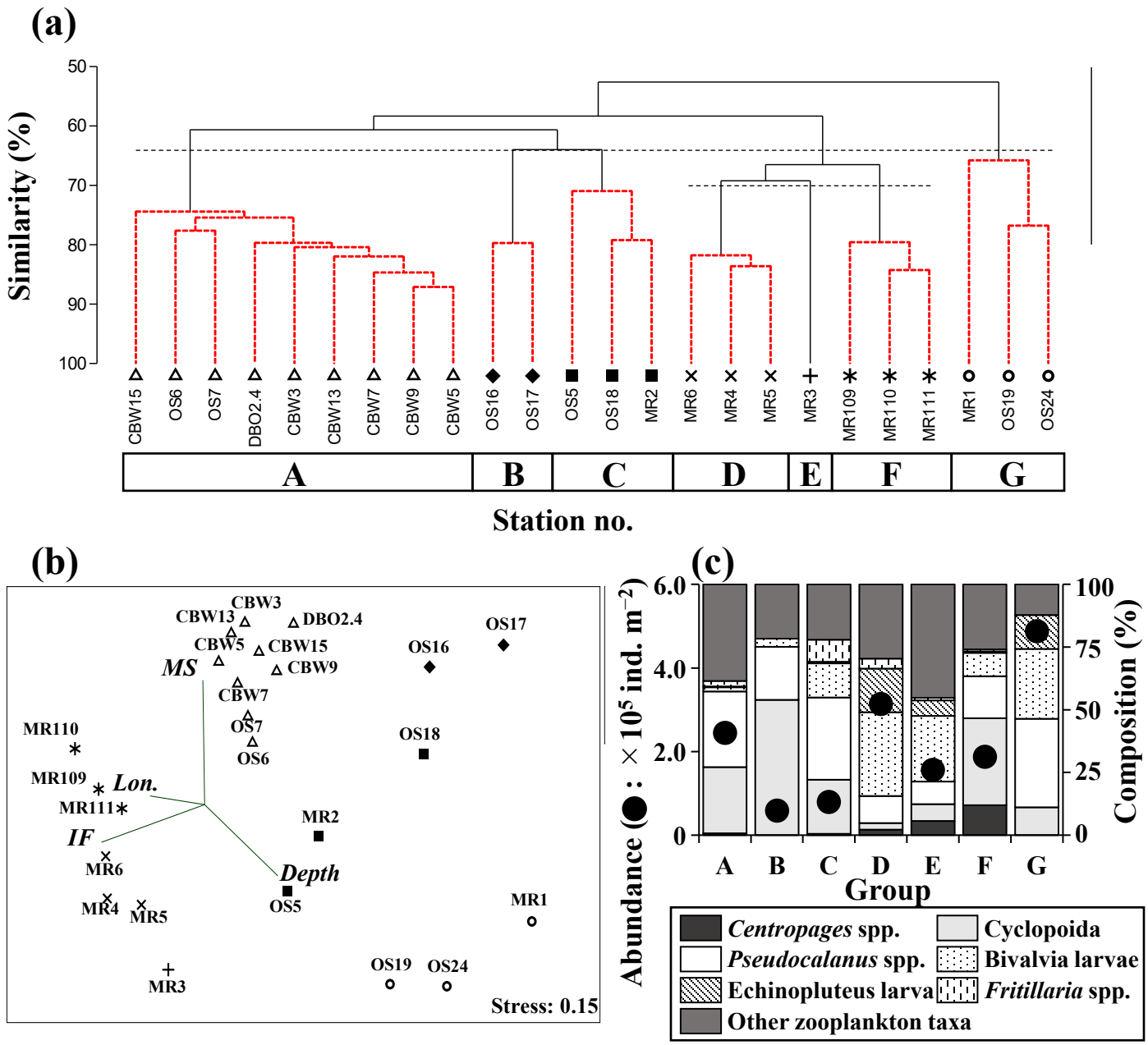

Fig. 5. (a) Dendrogram showing Bray-Curtis similarity results for zooplankton abundance. Eight groups (A-G) were identified at 64 and 70% similarity. (b) Nonmetric multidimensional scaling plots of the seven groups, with arrows indicating directions of environmental parameters. (c) The mean abundance and taxonomic composition of each group; only groups with a high % composition are separated. *Depth*: sampling depth (5 m off of the sea floor), *IF:* integrated water column fluorescence, *MS*: mean water column salinity, *Lon.*: longitude.

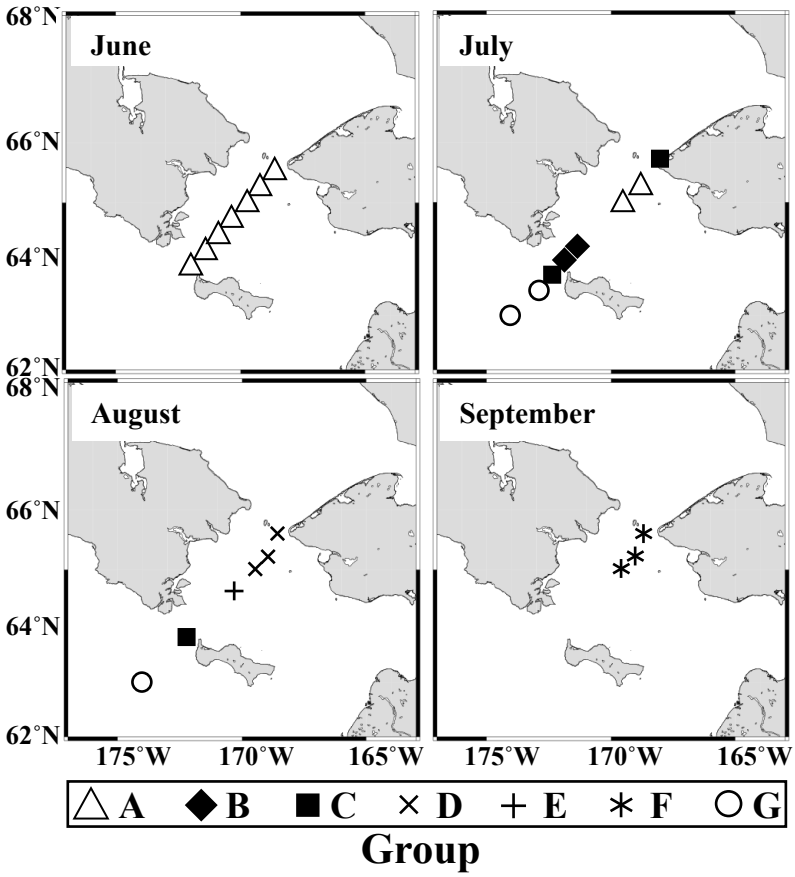

Fig. 6. Horizontal distributions of the seven station groups identified using Bray-Curtis similarity cluster analysis based on zooplankton abundance (cf. Fig. 5a) in the northern Bering Sea during June through September, 2017.

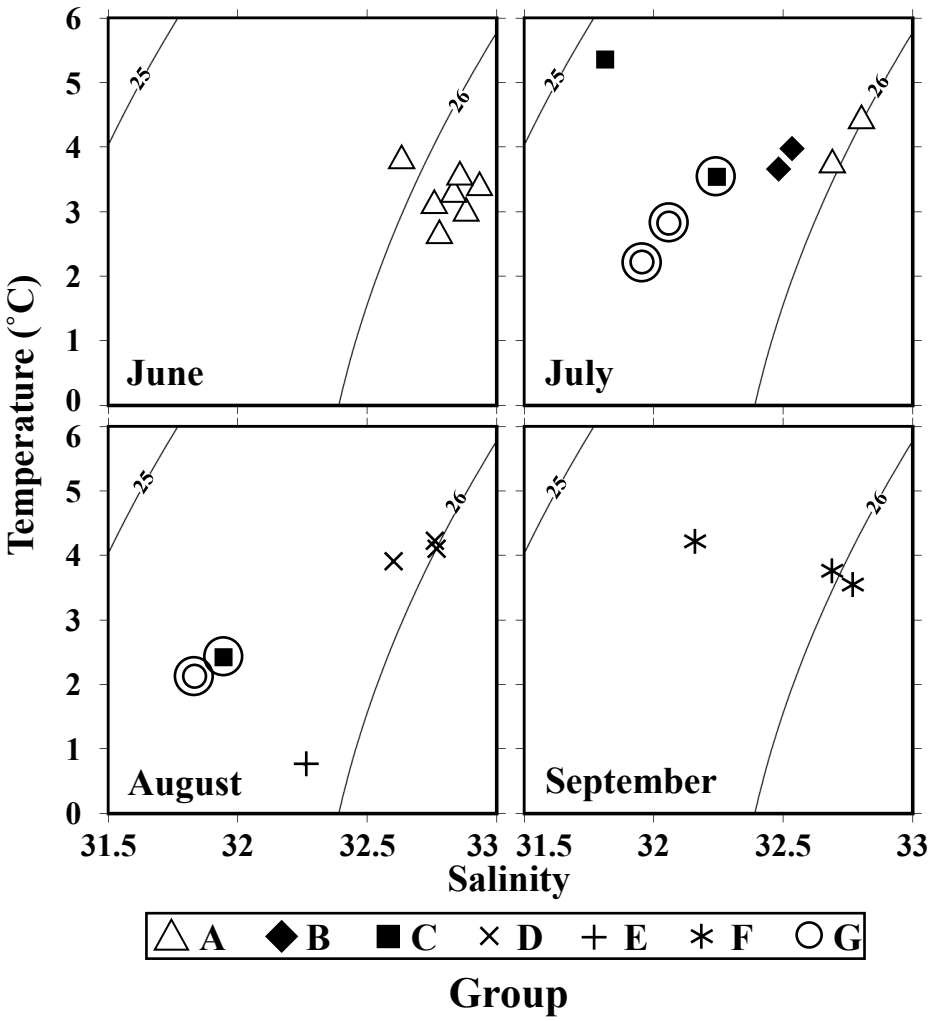

Fig. 7. T-S diagram with the seven groups identified from Bray-Curtis similarity based on zooplankton abundances (cf. Fig. 5a) in the northern Bering Sea during June through September of 2017. The plot position is mean values in the water column. Circles indicate that the stations were located west of 172° W.

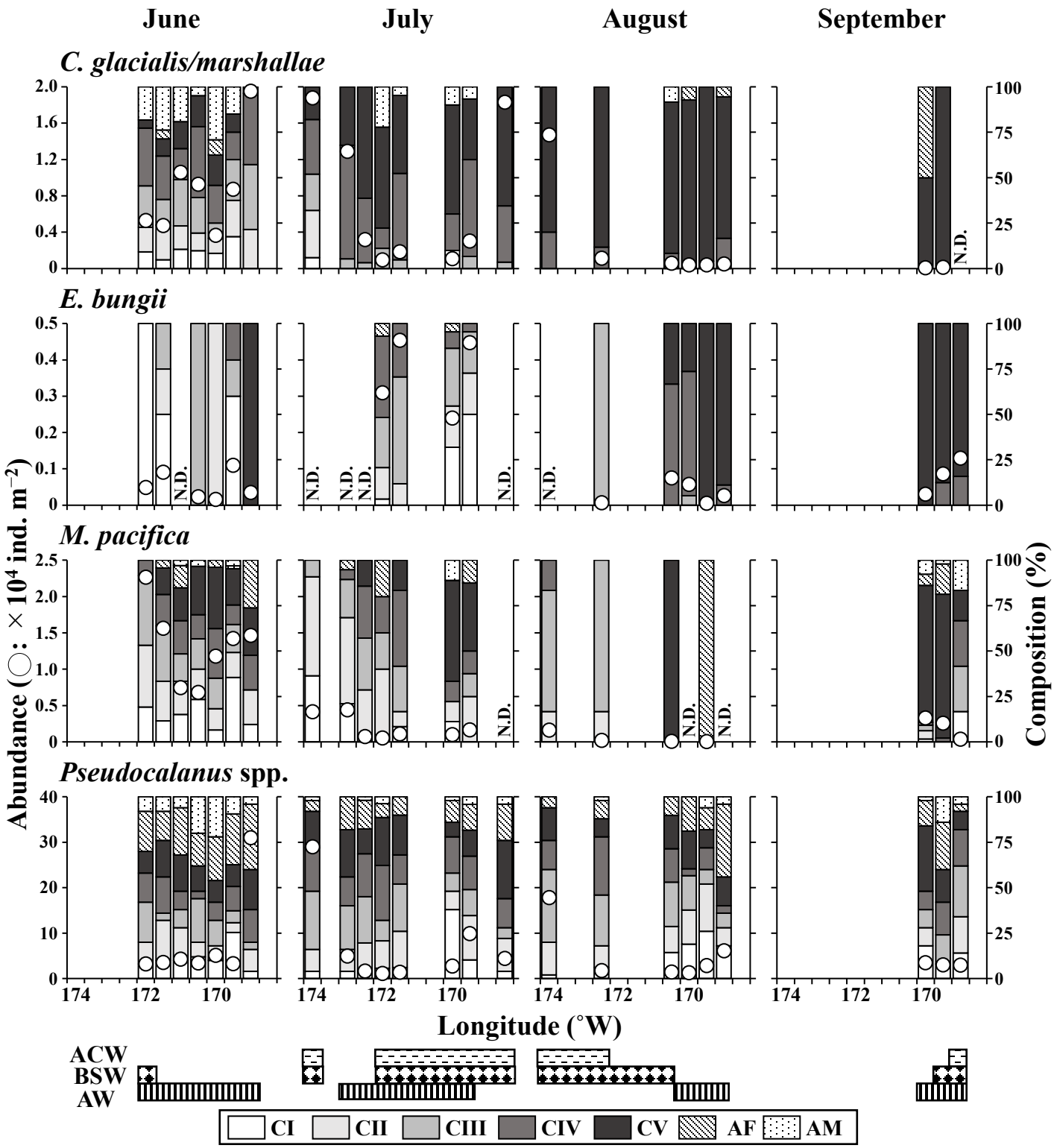

Fig. 8. Monthly changes in abundance and population structure for the dominant copepods in the northern Bering Sea during June through September, 2017. Horizontal bars below the plots indicate the water masses (ACW, BSW and AW) were present for each station.

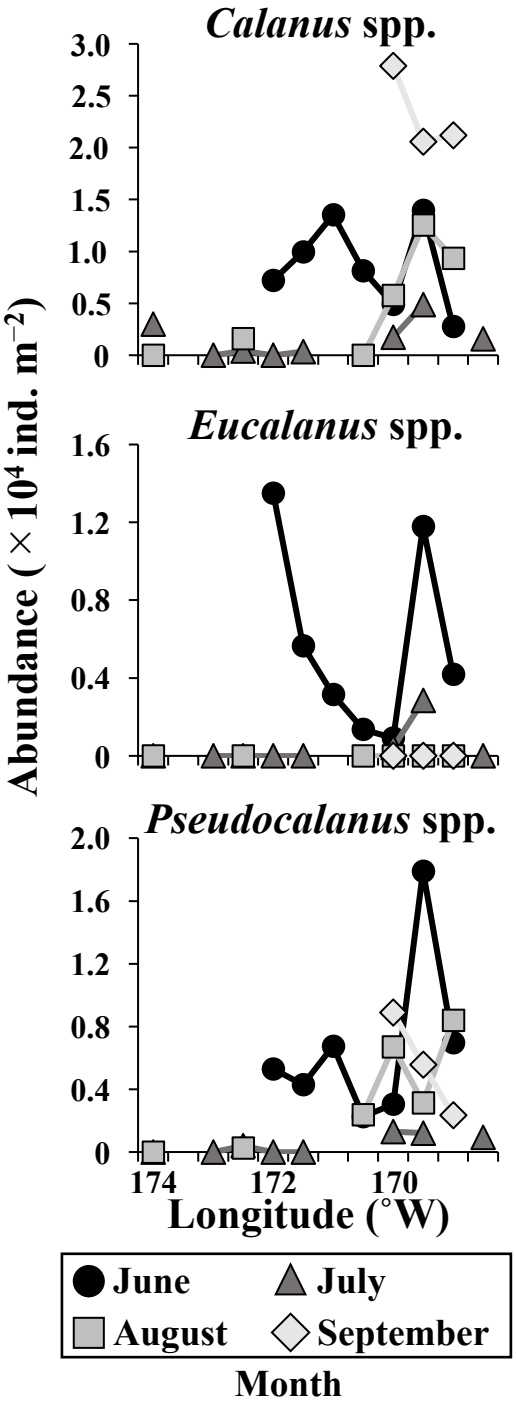

Fig. 9. Monthly changes in abundance of nauplii of the dominant copepods species in the northern Bering Sea during June through September, 2017.

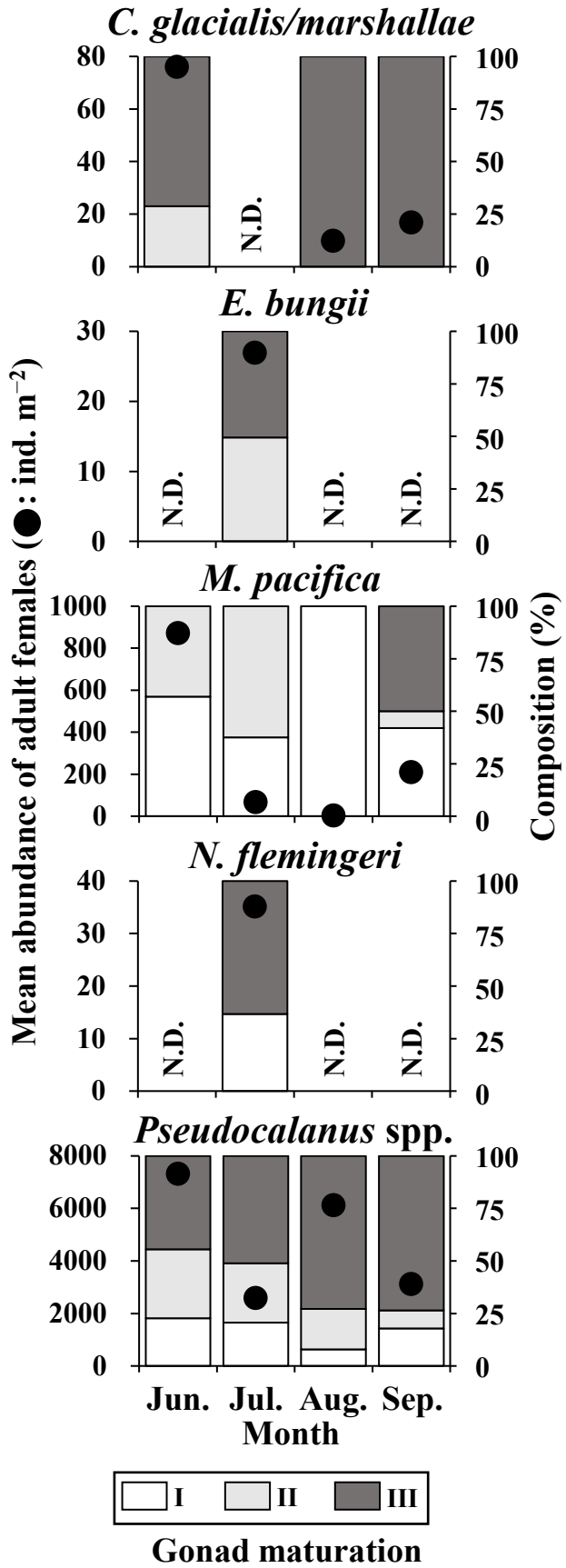

Fig. 10. Monthly changes in abundance and gonad maturation for adult females of the dominant copepods in the northern Bering Sea during June through September, 2017.

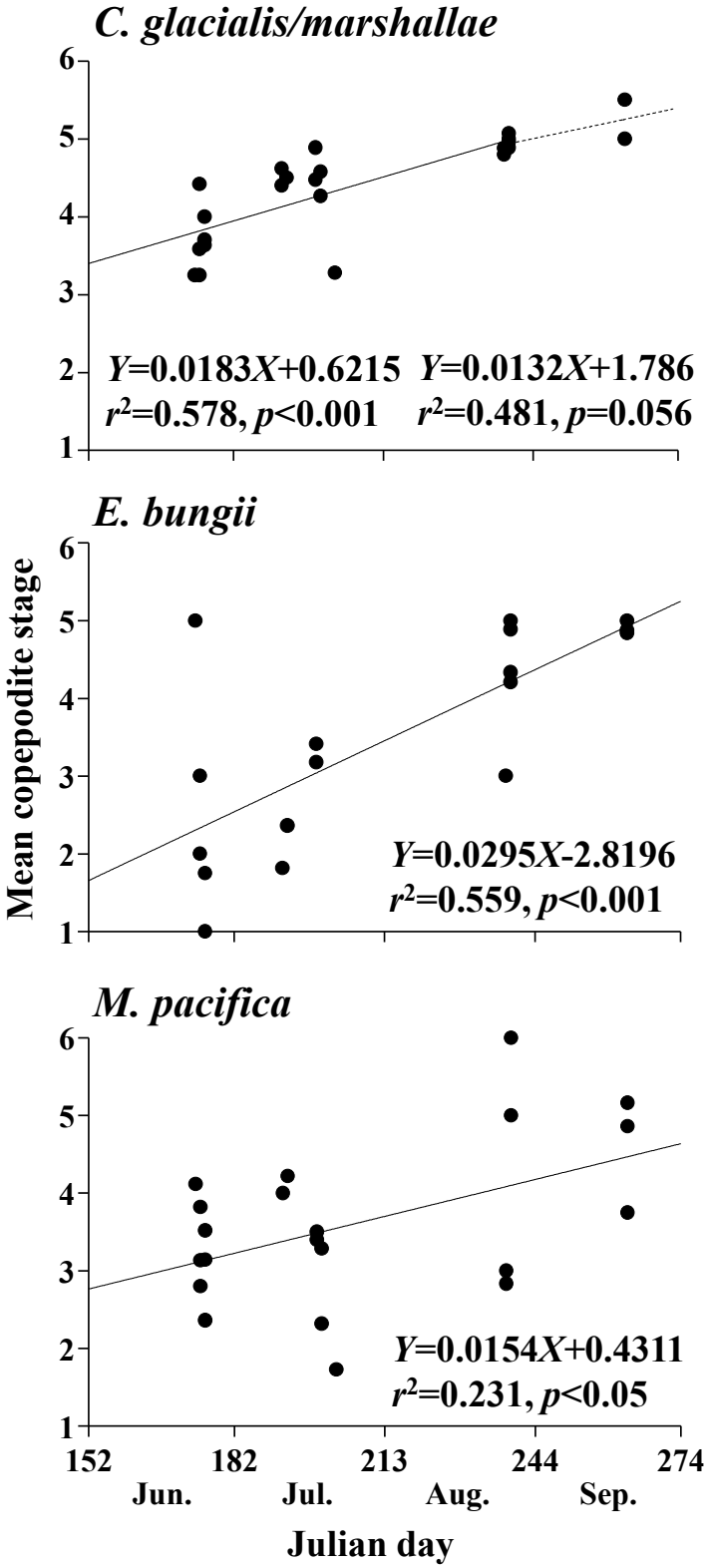

Fig. 11. Relationships between mean copepodite stage and Julian day for the dominant copepods in the northern Bering Sea during June through September, 2017.

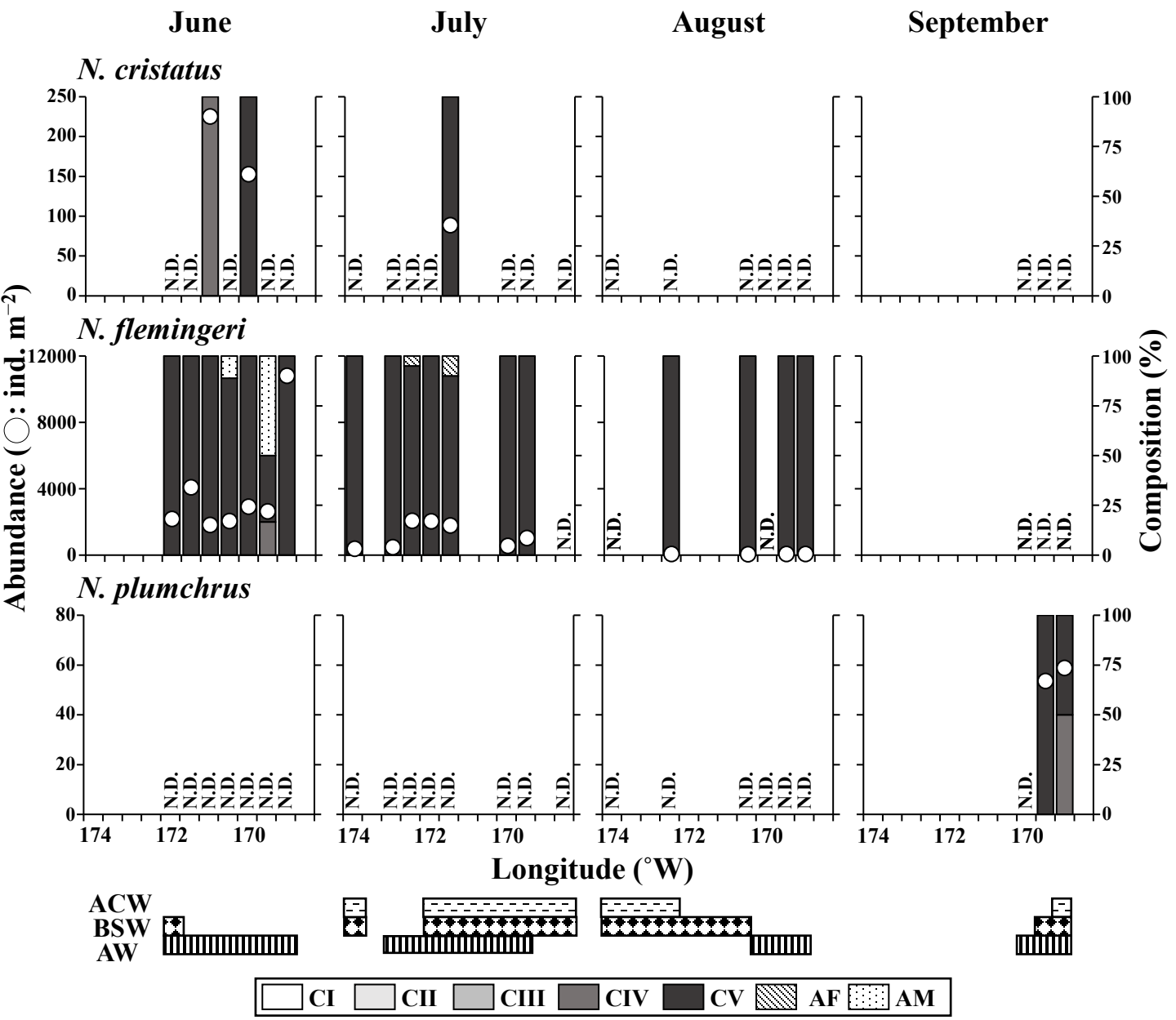

Fig. 12. Monthly changes in abundance and population structure for the Neocalanus species in the northern Bering Sea during June through September, 2017. Horizontal bars below the plots indicate the water masses (ACW, BSW and AW) present for each station.

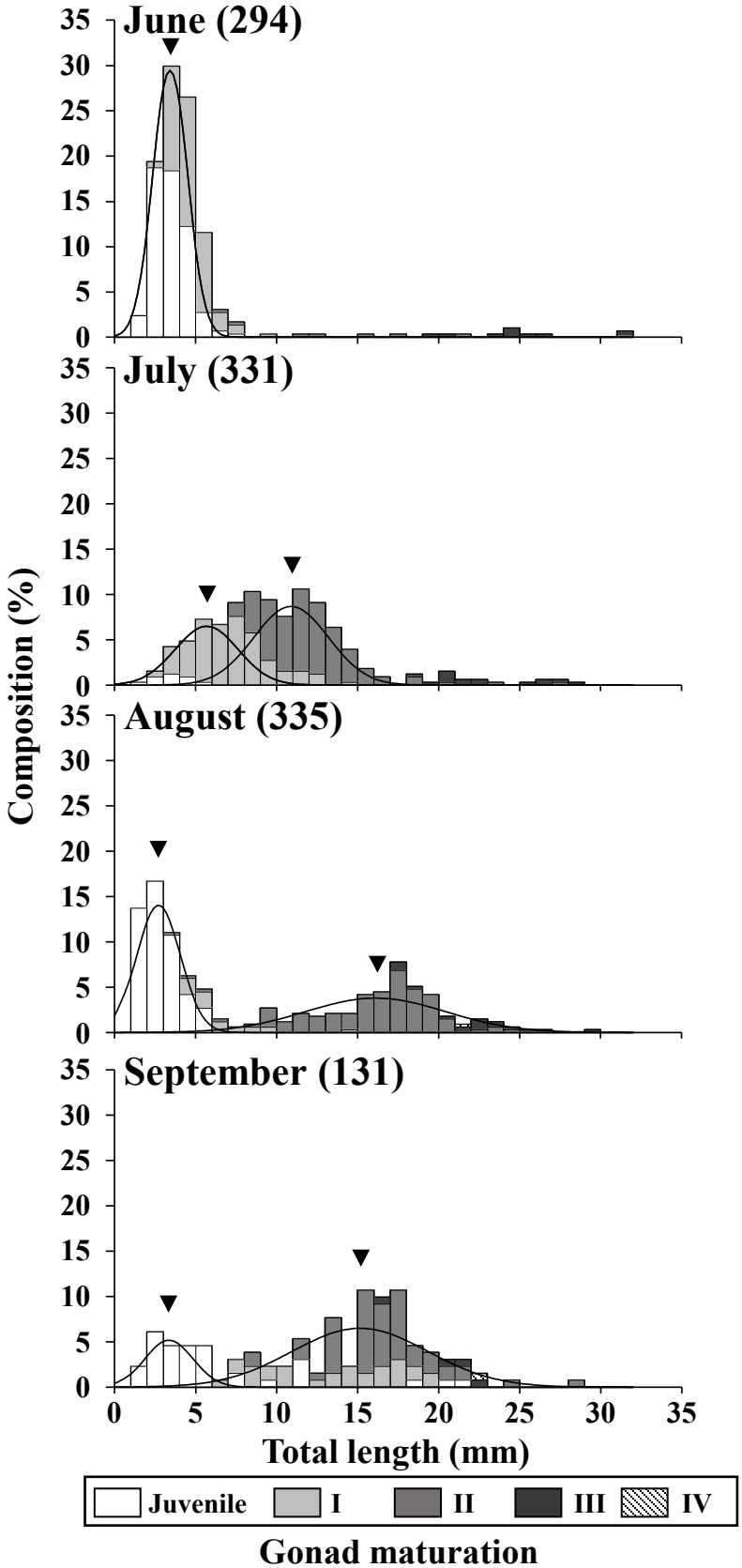

Fig. 13. Monthly changes in the total length of Parasagitta elegans in the northern Bering Sea during June through September, 2017. Numbers in parentheses show total individual measurements. Smooth curves indicate the results of a cohort analysis.

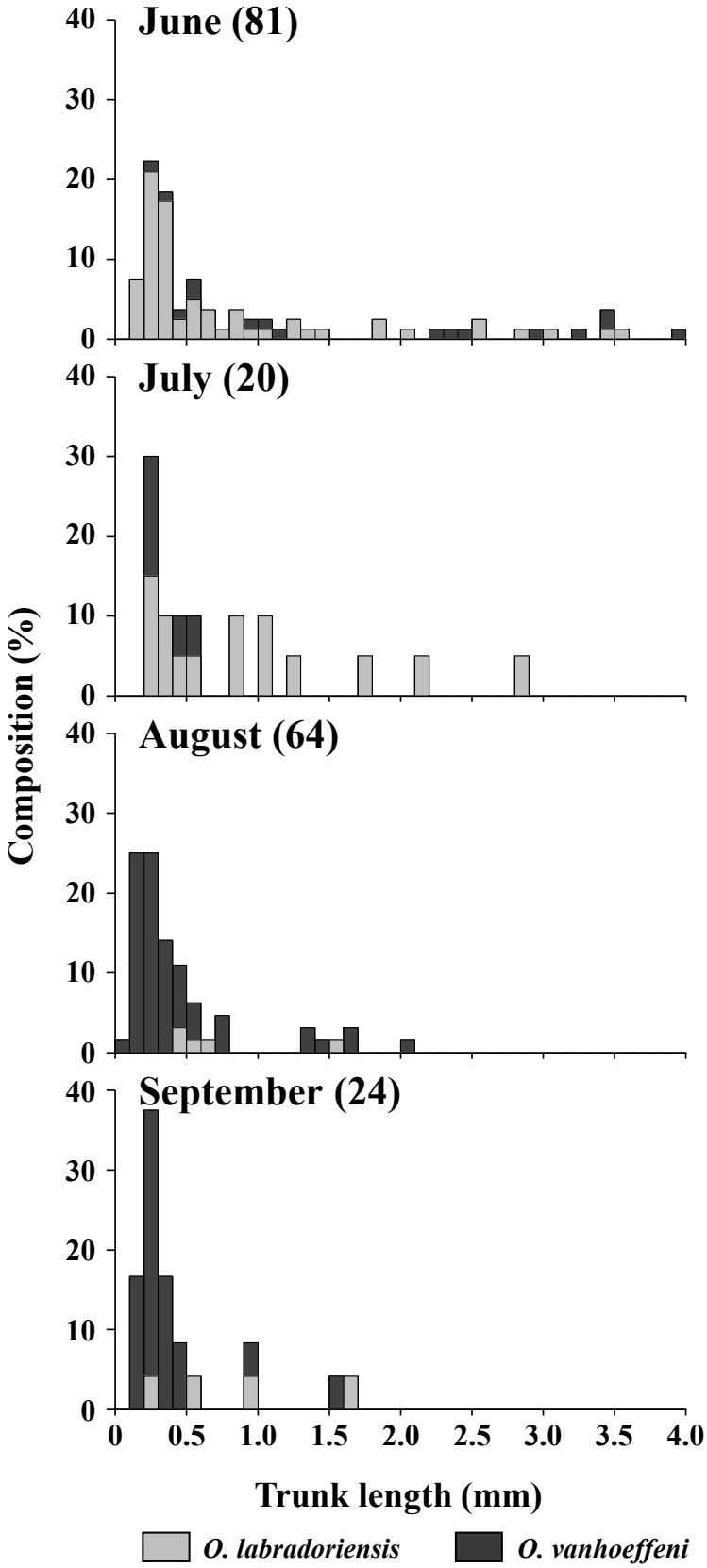

Fig. 14. Monthly changes in the trunk length of Oikopleura spp. in the northern Bering Sea during June through September 2017. Numbers in parentheses show total individual measurements.